Proton Capture on Carbon Isotopes

$^{12}C(p,\gamma)^{13}N$ and $^{13}C(p,\gamma)^{14}N$ at LUNA

Jakub Skowronski [1,2]

[1] Università degli Studi di Padova

[2] Istituto Nazionale di Fisica Nucleare, Sezione di Padova

16th Varenna Conference on Nuclear Reaction Mechanisms

Astrophysical Motivation

- Two reactions of the **CNO cycle**
- They govern the **amount** of **^{12}C** and **^{13}C** in **stellar cores**

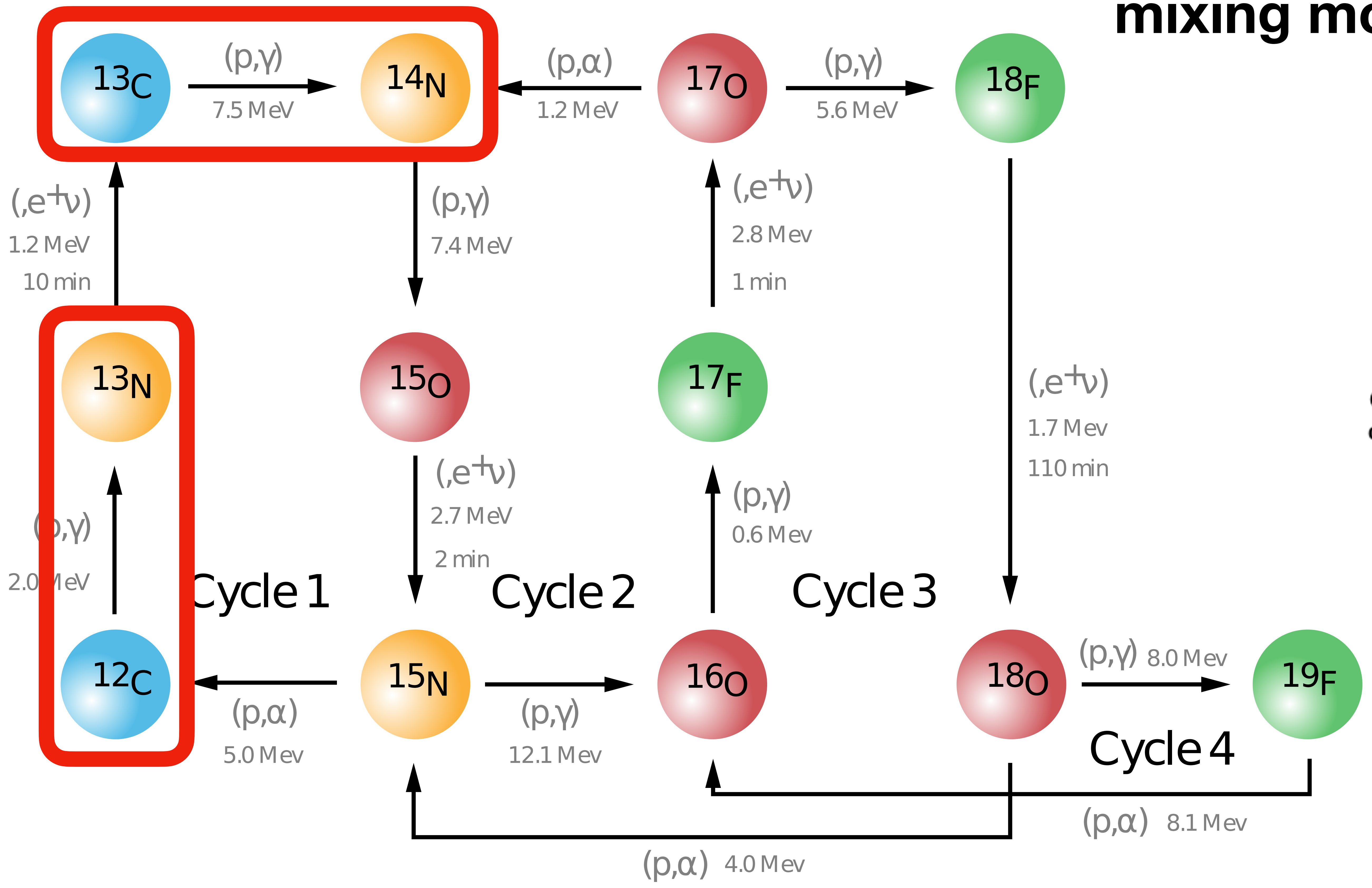

- The **^{12}C/^{13}C** ratio can be **obtained from stellar spectra**
- Asymptotic Giant Branch (**AGB**) stars undergo **heavy mixing**
- A precise ^{12}C/^{13}C ratio in the core can help to **constrain the mixing models**

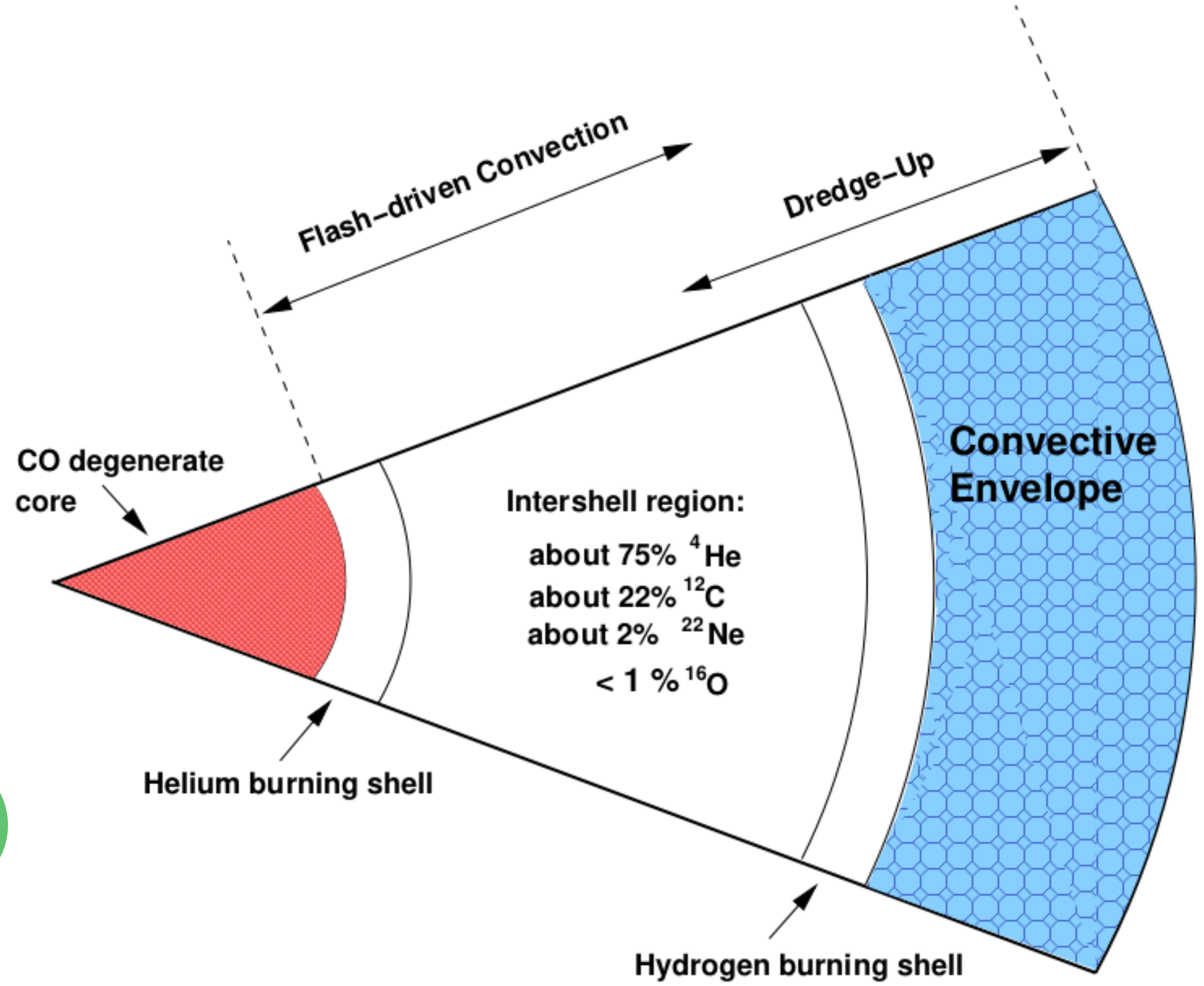

LUNA

$^{12}C(p,\gamma)^{13}N$ Reaction

$^{12}C + p \rightarrow {}^{13}N + \gamma$ (Q = 1.943 MeV)

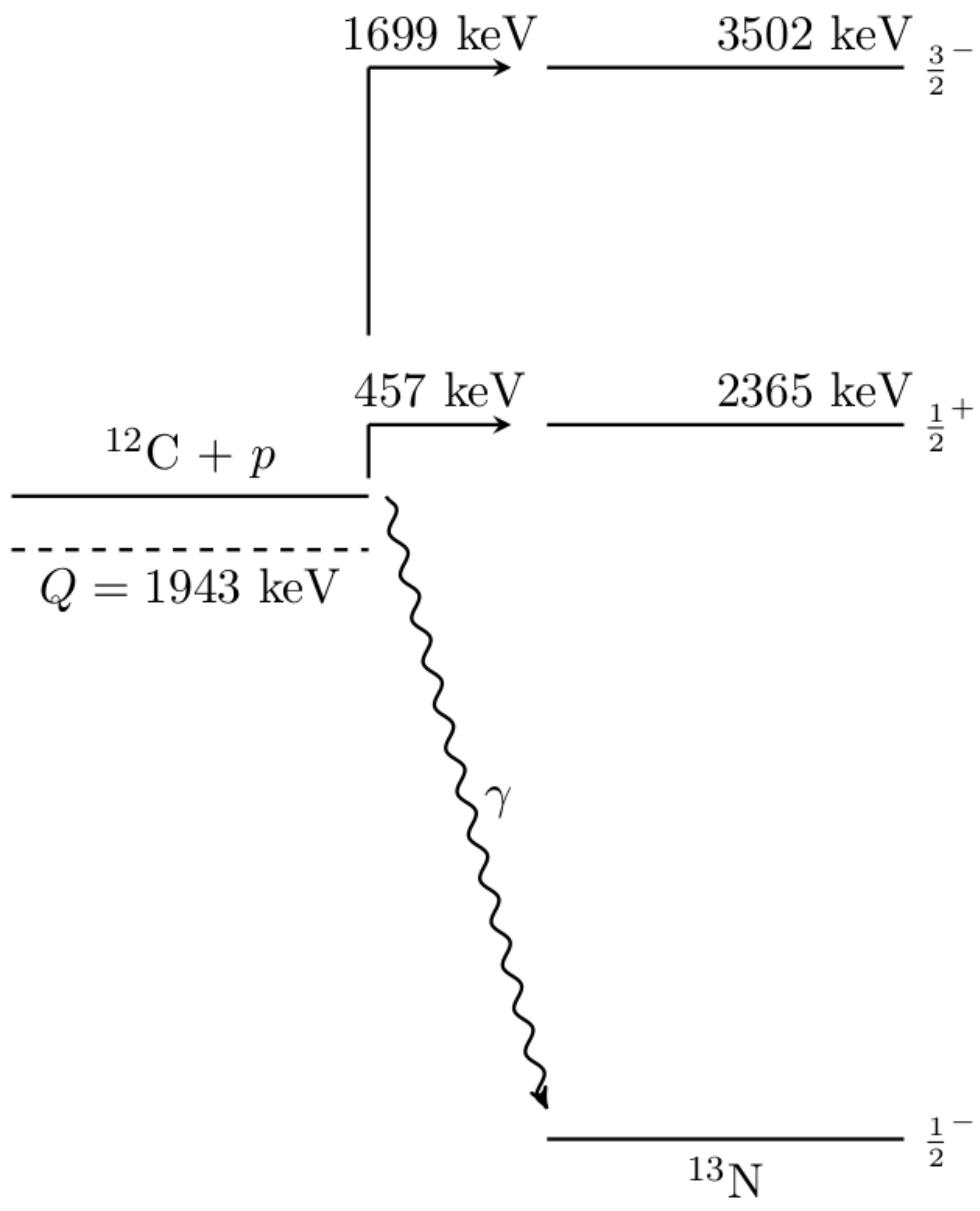

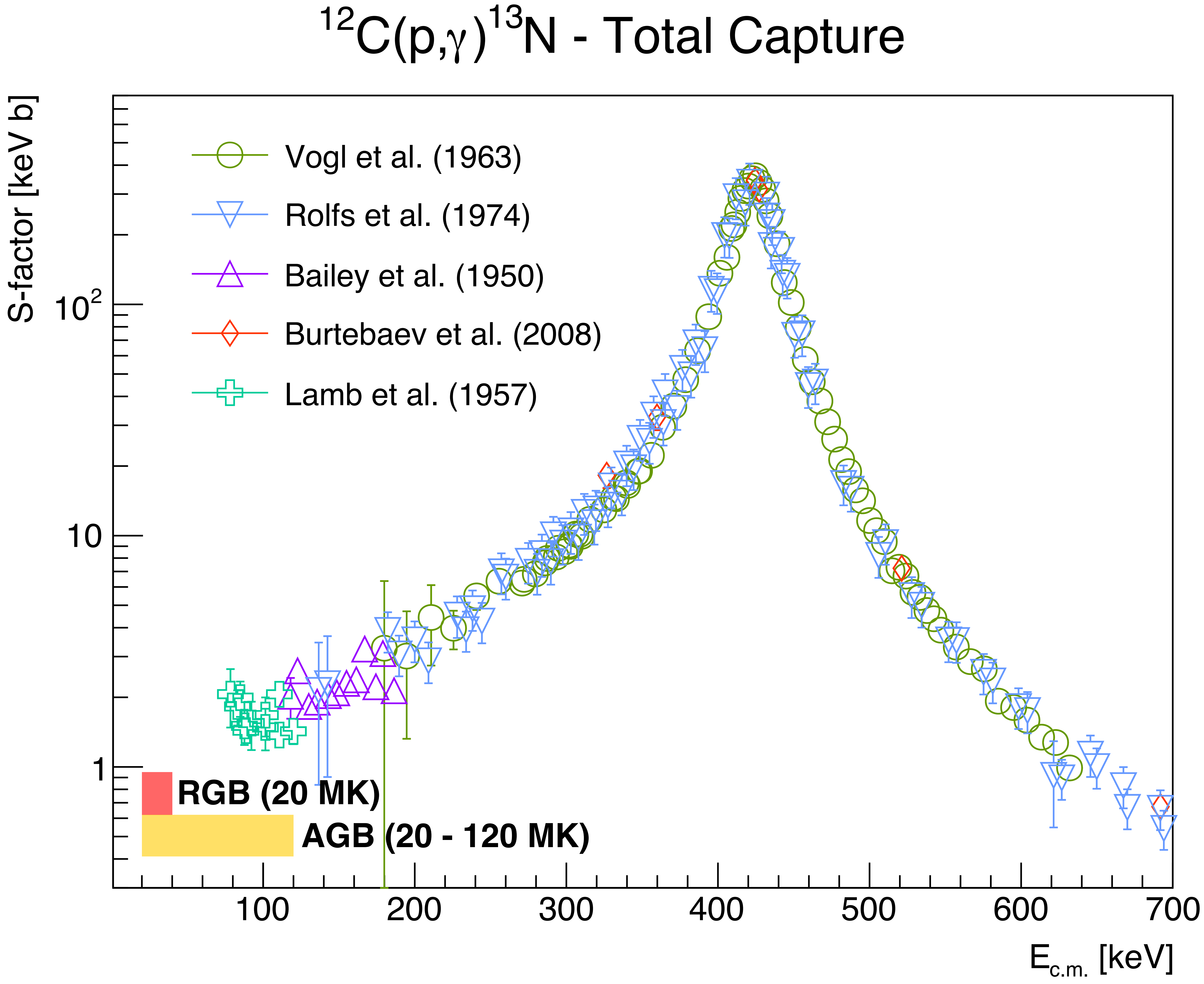

$^{13}C(p,\gamma)^{14}N$ Reaction

$^{13}C + p \rightarrow {}^{14}N + \gamma$ (Q = 7.551 MeV)

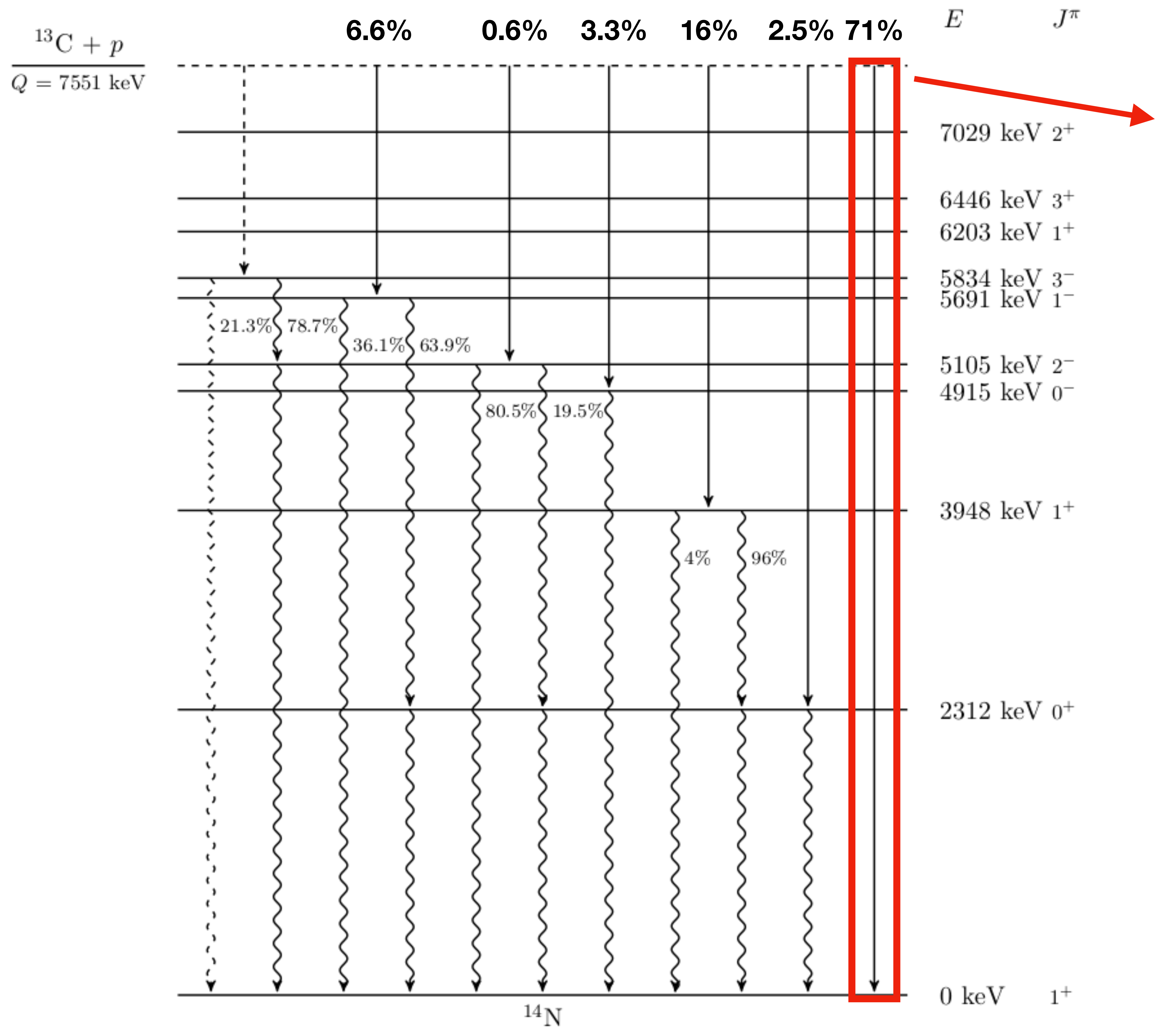

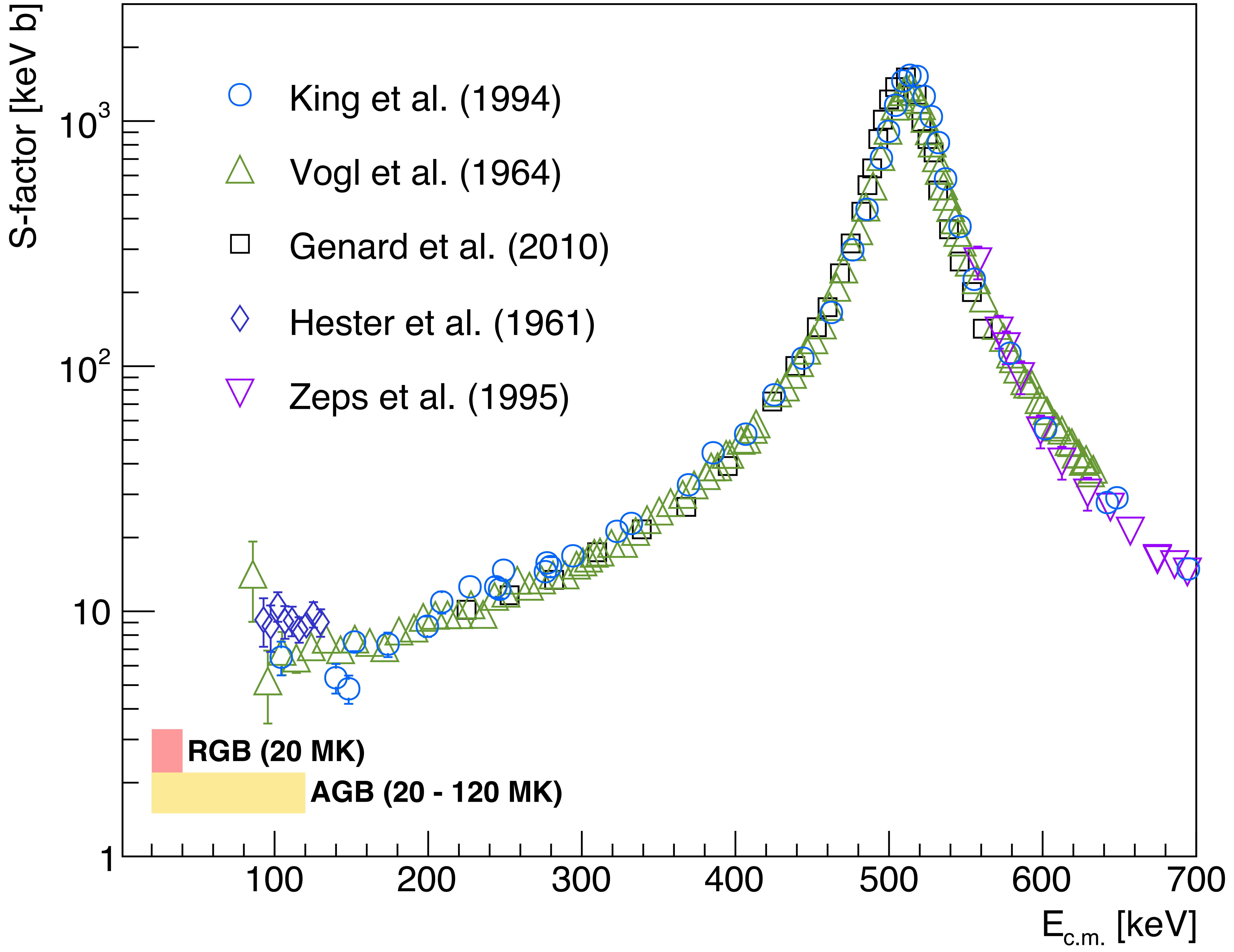

Laboratory for Underground Nuclear Astrophysics

- Located at LNGS facility under the **Gran Sasso mountain** in Abruzzo, Italy
- The cosmic ray flux reduced by **six orders of magnitude**

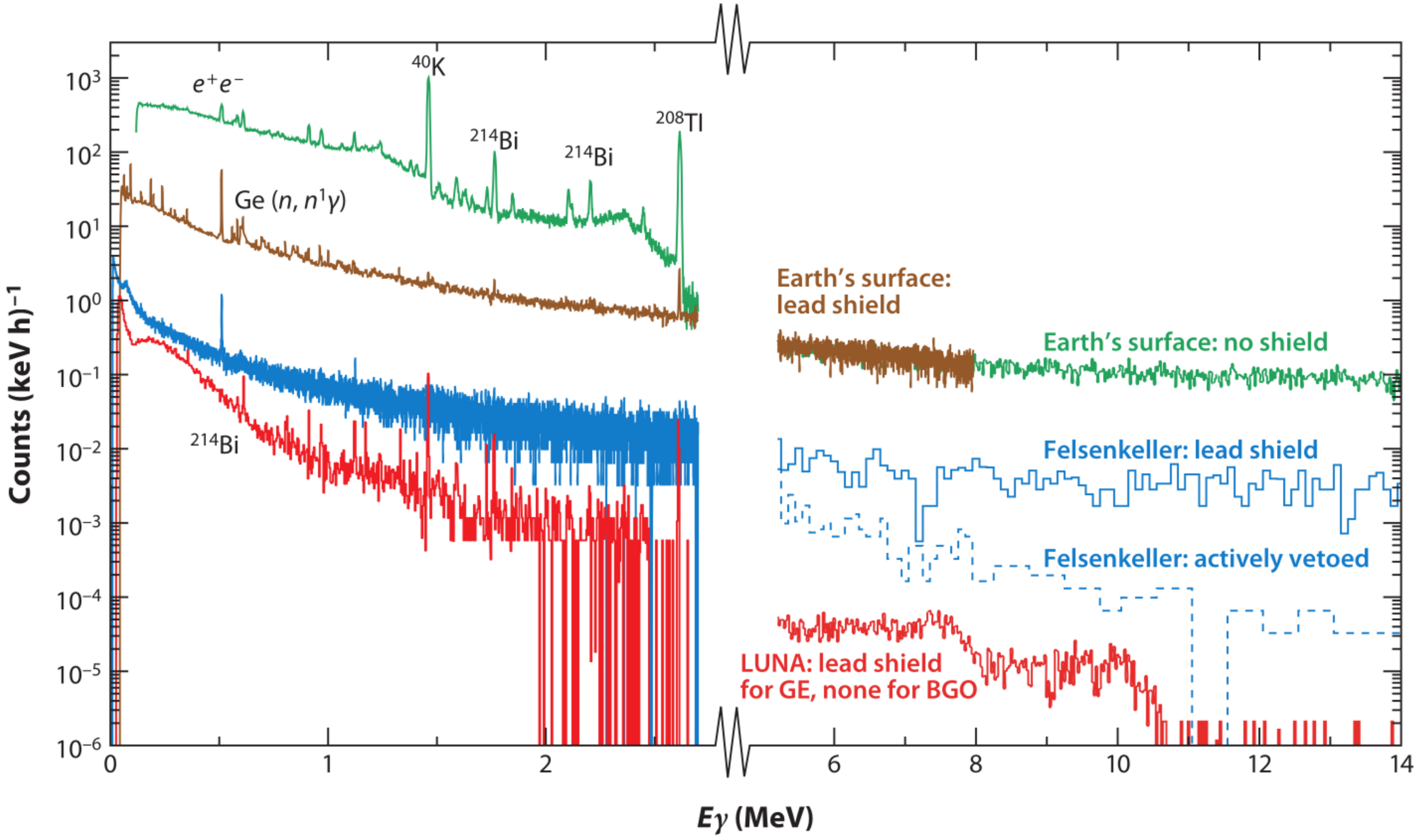

LUNA

Experimental Setup

Two different setups were used:

HPGe

- Close geometry (**1.4 cm**) at **0°**
- Far geometry (**15 cm**) at **55°**
- Excellent **energy resolution**

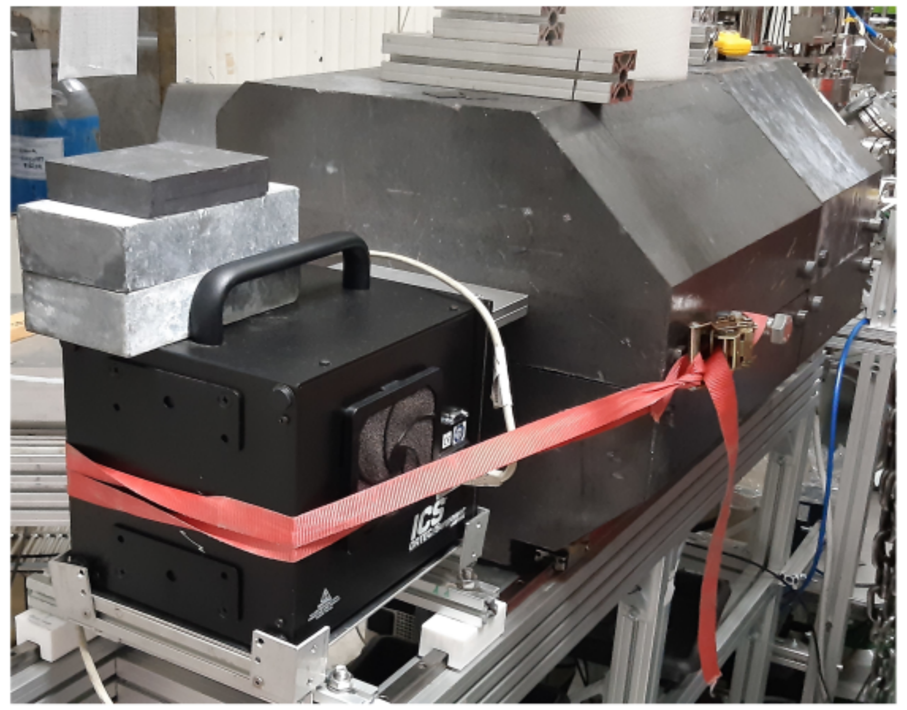

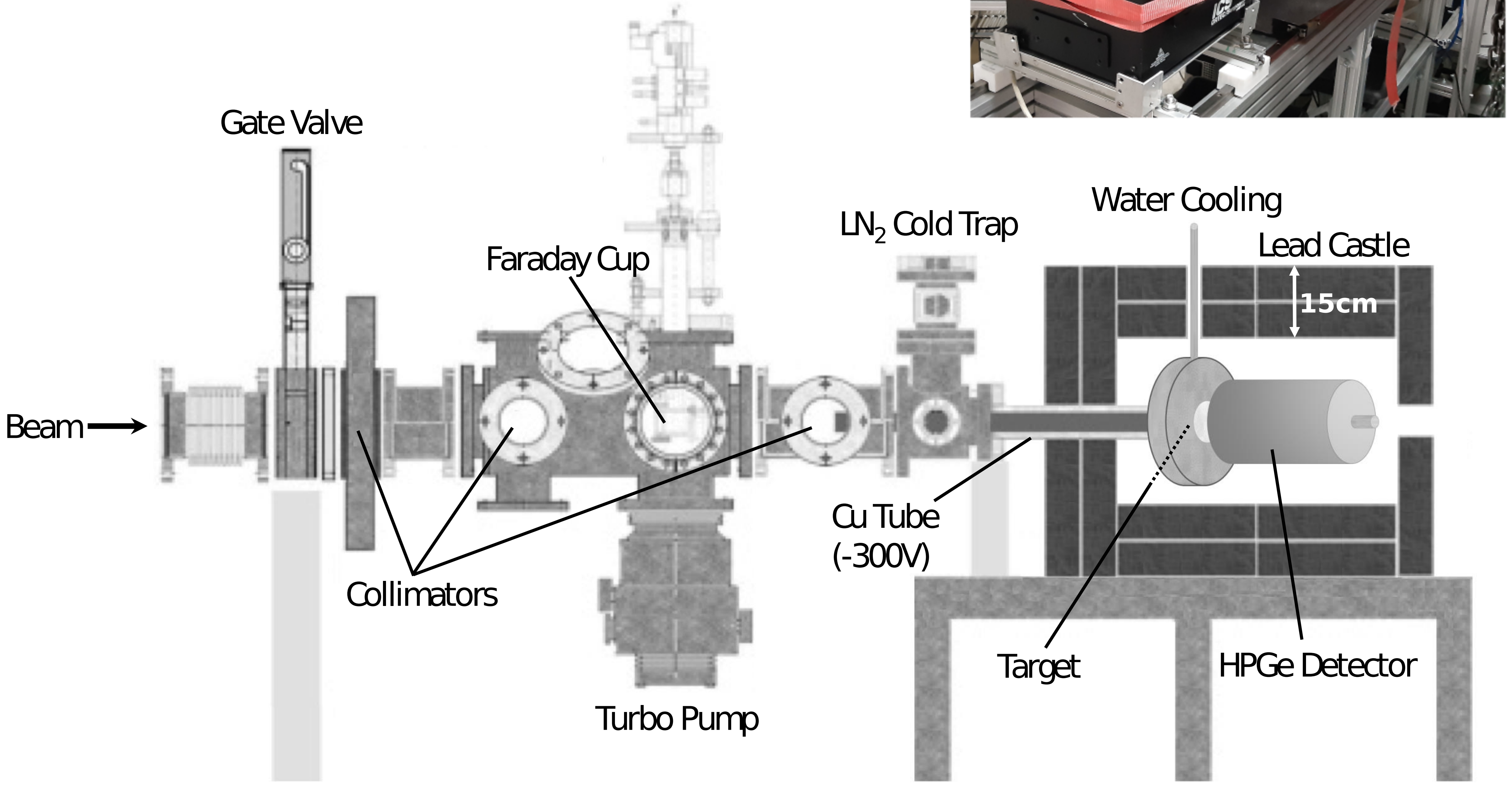

BGO

- Almost **4π geometry**
- Segmented in **6 different crystals**
- **Target check** with HPGe at 55°

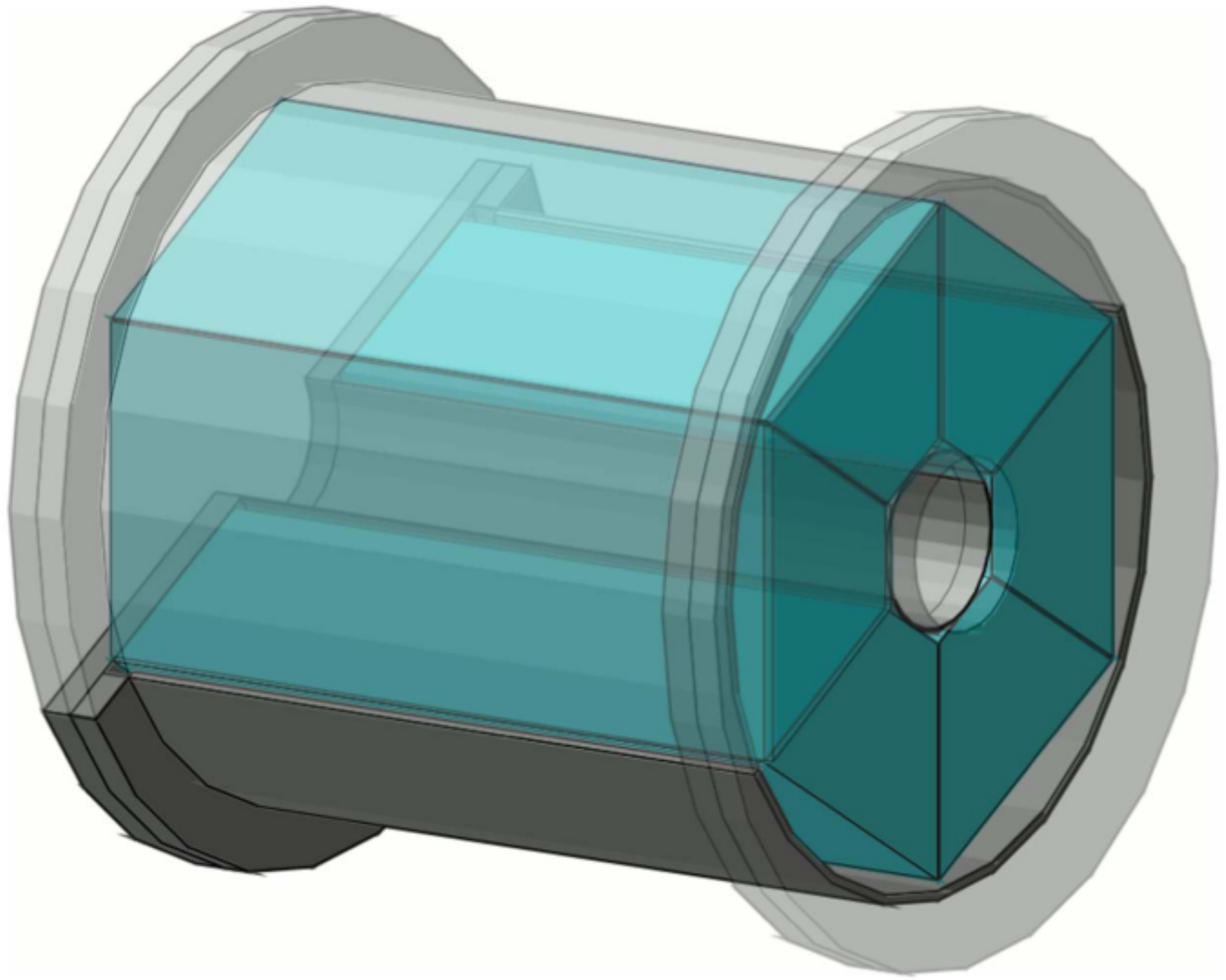

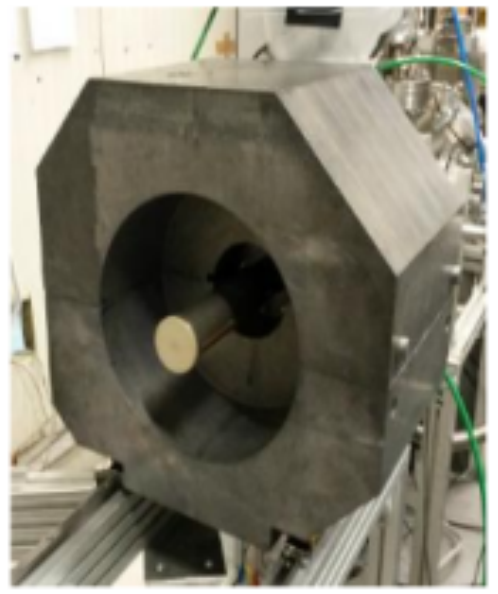

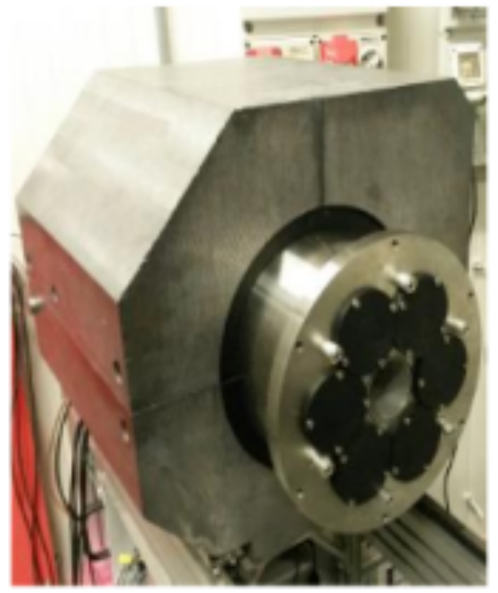

γ-Ray Spectra

HPGe

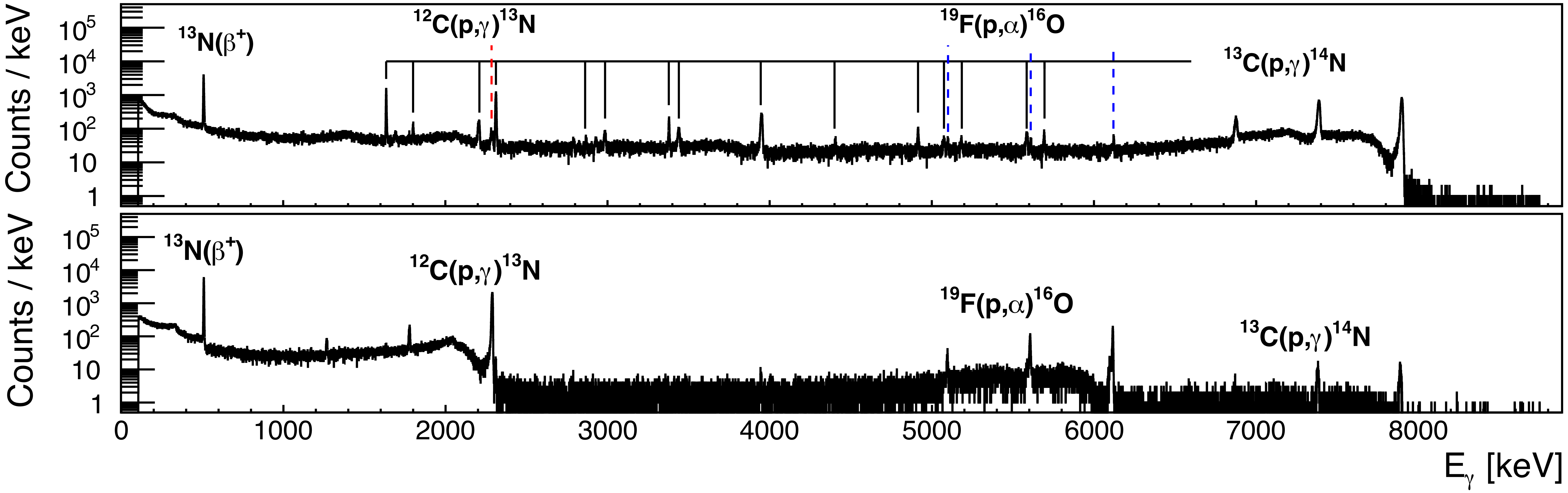

Target: 99% ^{13}C enriched

^{13}C(p,γ)^{14}N

Target: natural carbon

^{12}C(p,γ)^{13}N

BGO

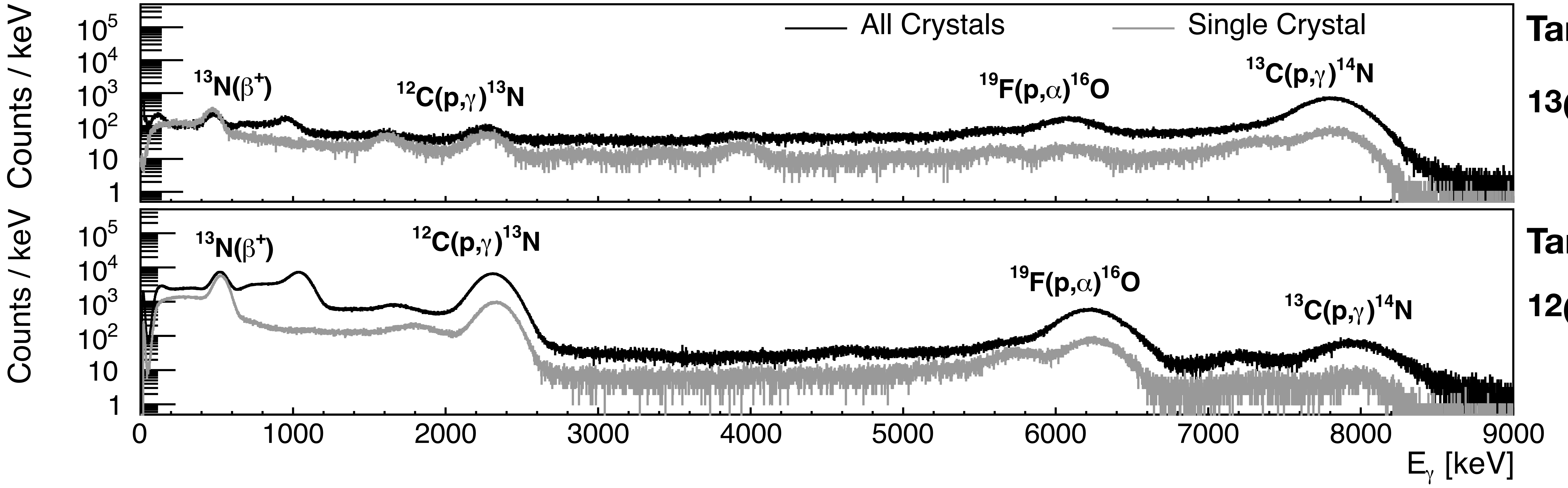

Target: 99% ^{13}C enriched

^{13}C(p,γ)^{14}N

Target: natural carbon

^{12}C(p,γ)^{13}N

Peak Shape Analysis

- **Shape** of the **γ-peak** depends on **target thickness** and **cross section**
- **By proper parametrisation,** It is possible to **extract** both the **cross section** and the **target profile**

$$N_i = P(E_{p,i}) \frac{\sigma(E_{p,i})}{\epsilon_{\text{eff}}(E_{p,i})} \eta_{ph}(E_{\gamma,i}) W(\theta, E_p) N_p \Delta E_{\gamma,i}$$

Counts — Target Profile — Cross Section — Stopping Power — Efficiency — Angular Distribution — Current — Binning

Target: evaporated
Energies: 80 - 400 keV
Systematic: 7.1%

Method explained in:

G. F. Ciani et al. (2020), Eur. Phys. J. A, **56** 75

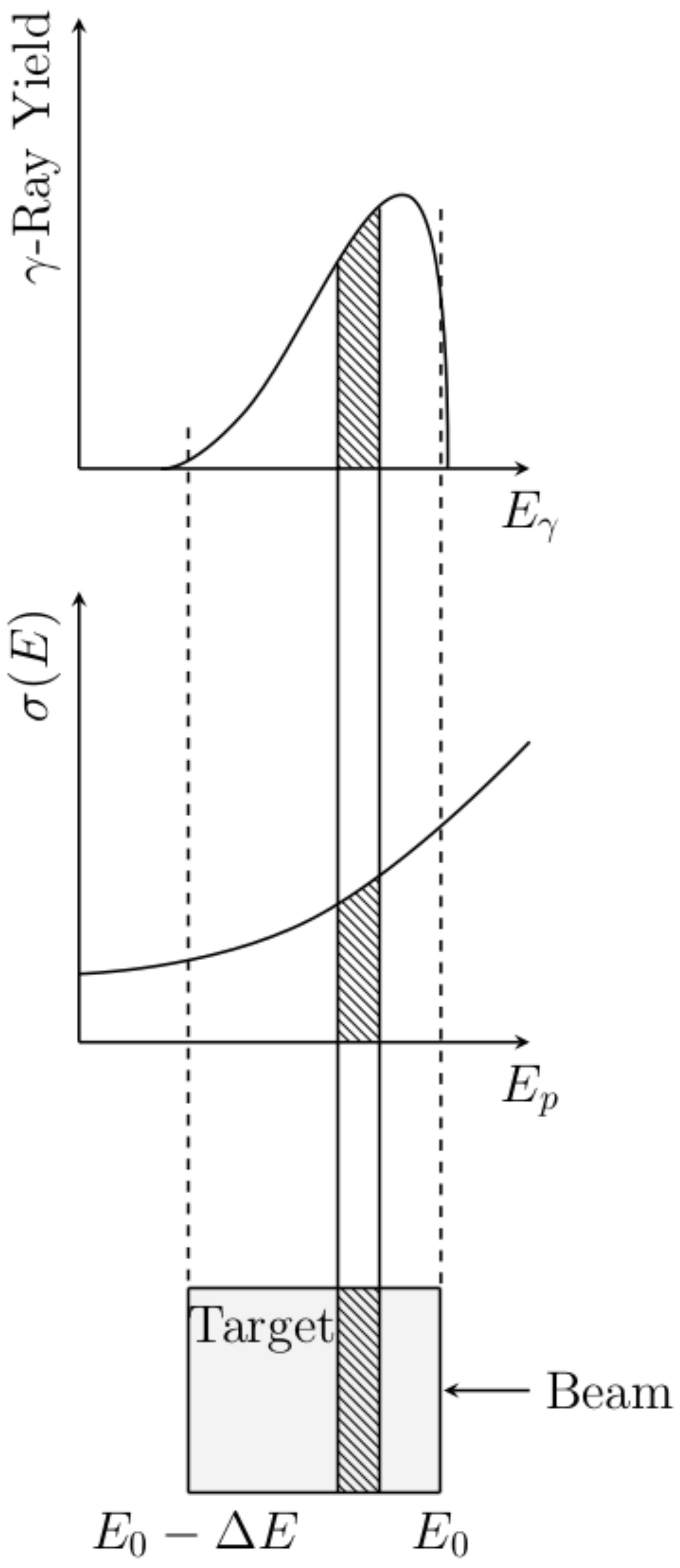

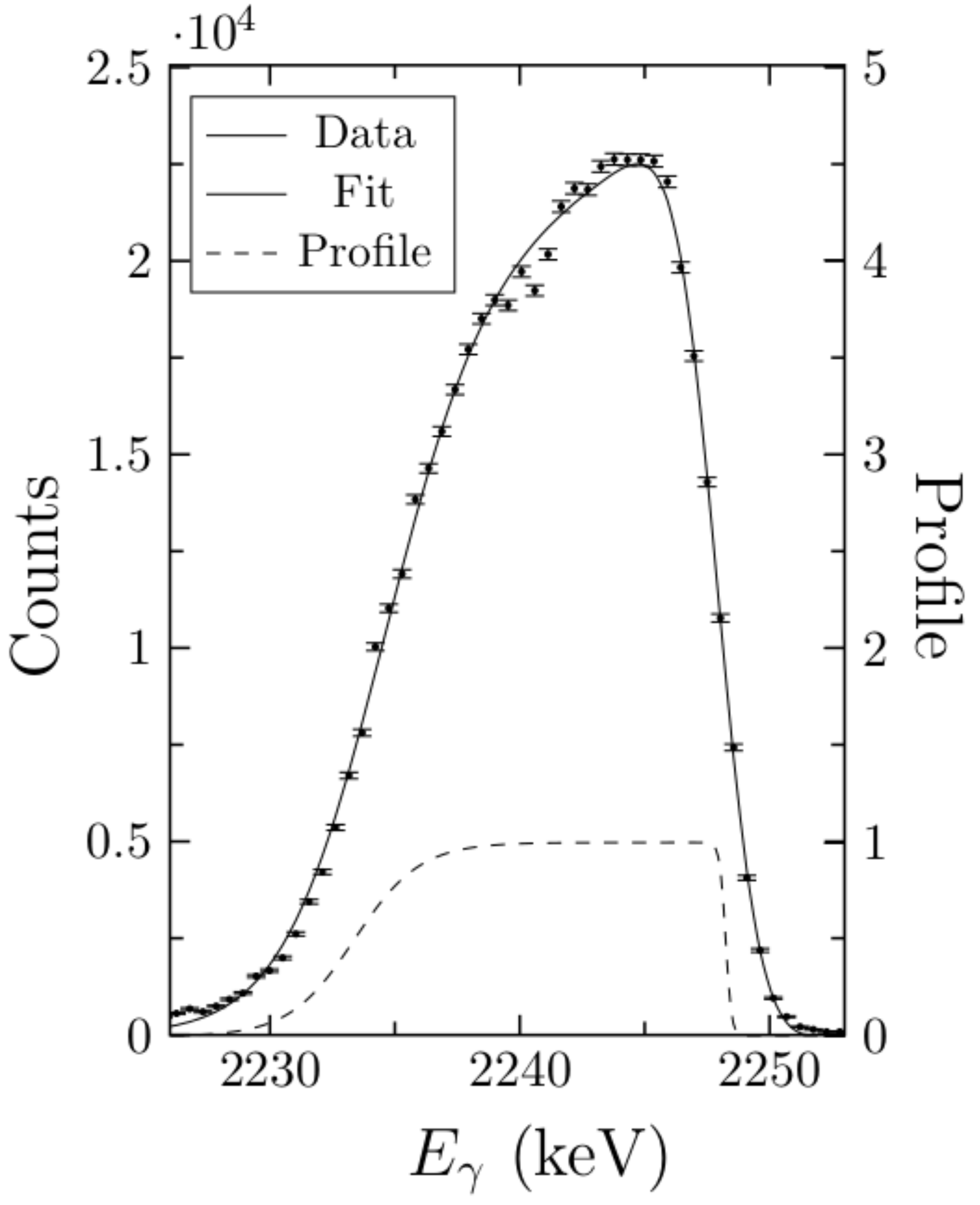

BGO Measurement

$^{12}C(p,\gamma)^{13}N$ - Activation Counting

- The produced ^{13}**N** is **β⁺ unstable** ($t_{1/2}$ = 9.965 min)
- Counting the **511 keV** in **opposite BGO crystals**

Target: 4 mm graphite disk
Energies: 80 - 400 keV
Systematic: 8.2%

Method explained in:

J. Skowronski et al. (2023), J. Phys. G: Nucl. Part. Phys. **50** 045201

$^{12}C(p,\gamma)^{13}N$ @ 150 keV

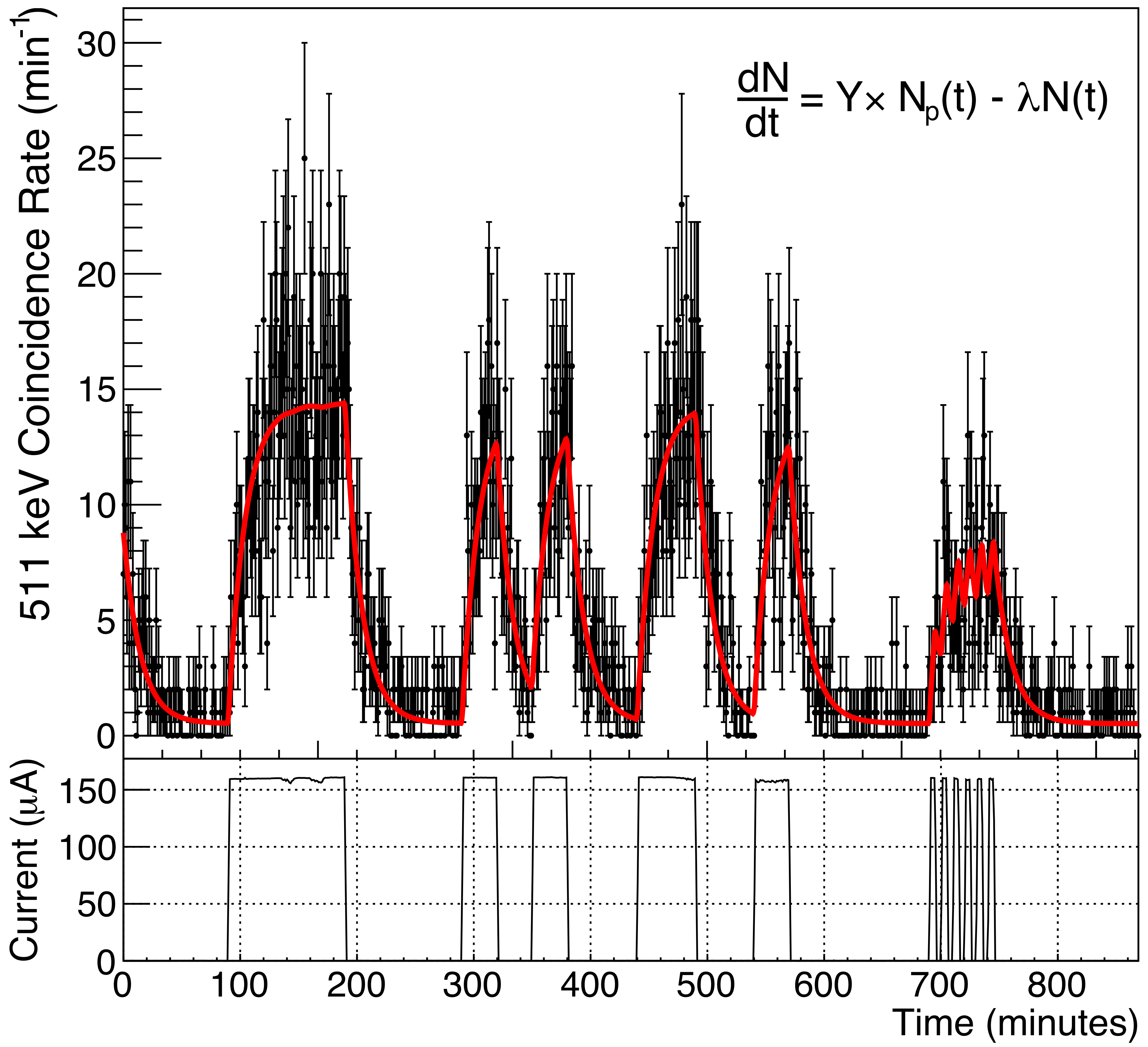

$^{12}C(p,\gamma)^{13}N$ - Total Capture

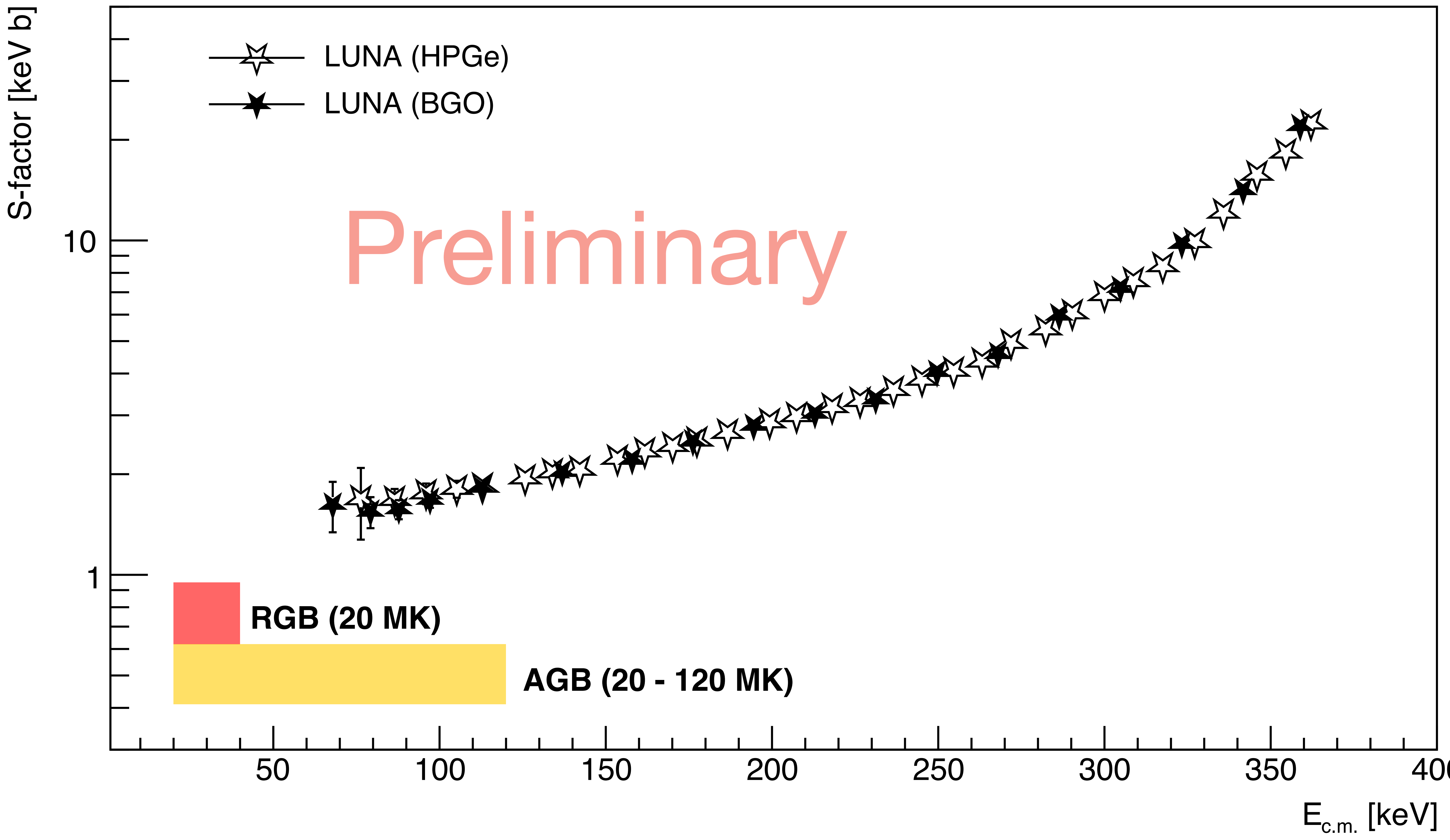

BGO Measurement

$^{13}C(p,\gamma)^{14}N$ - Total Absorption Spectroscopy

- Observing **all the γ-rays** from **all the crystals**
- High **Q-value** → **sum γ-peak** in background-less region

Target: evaporated
Energies: 60 - 400 keV
Systematic: 7.8%

Method explained in:

A. Boeltzig et al. (2018), J. Phys. G: Nucl. Part. Phys. **45** 025203

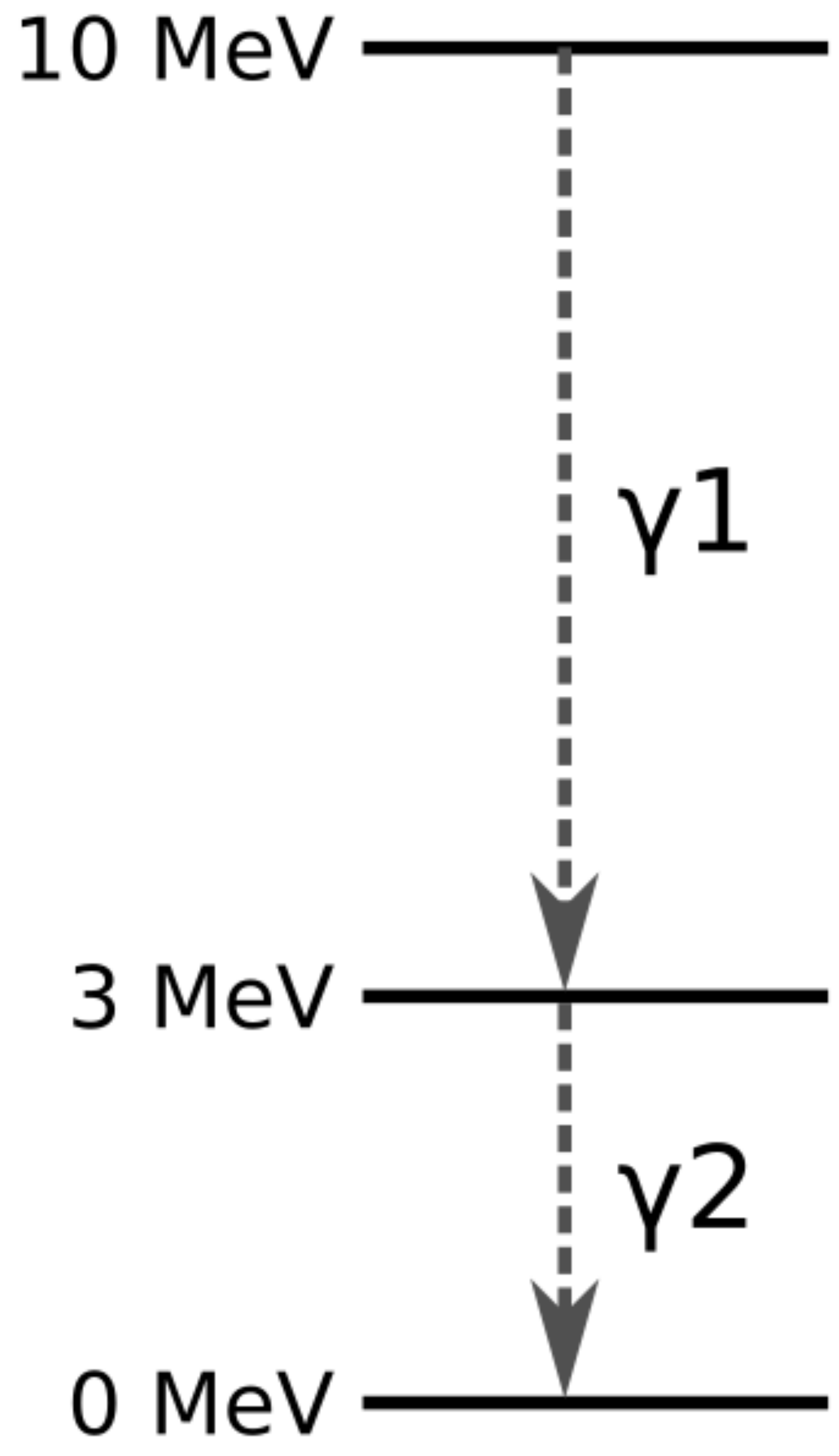

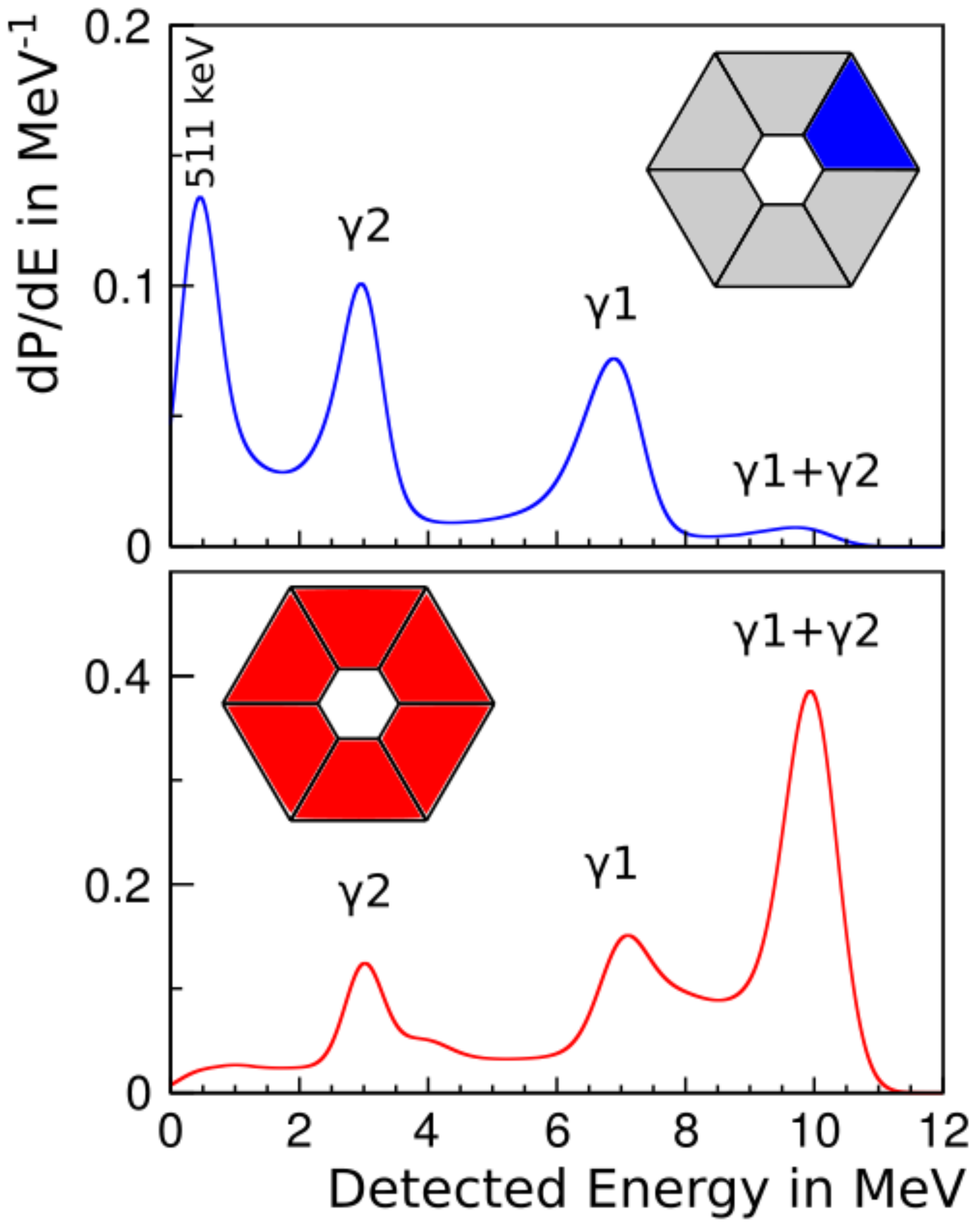

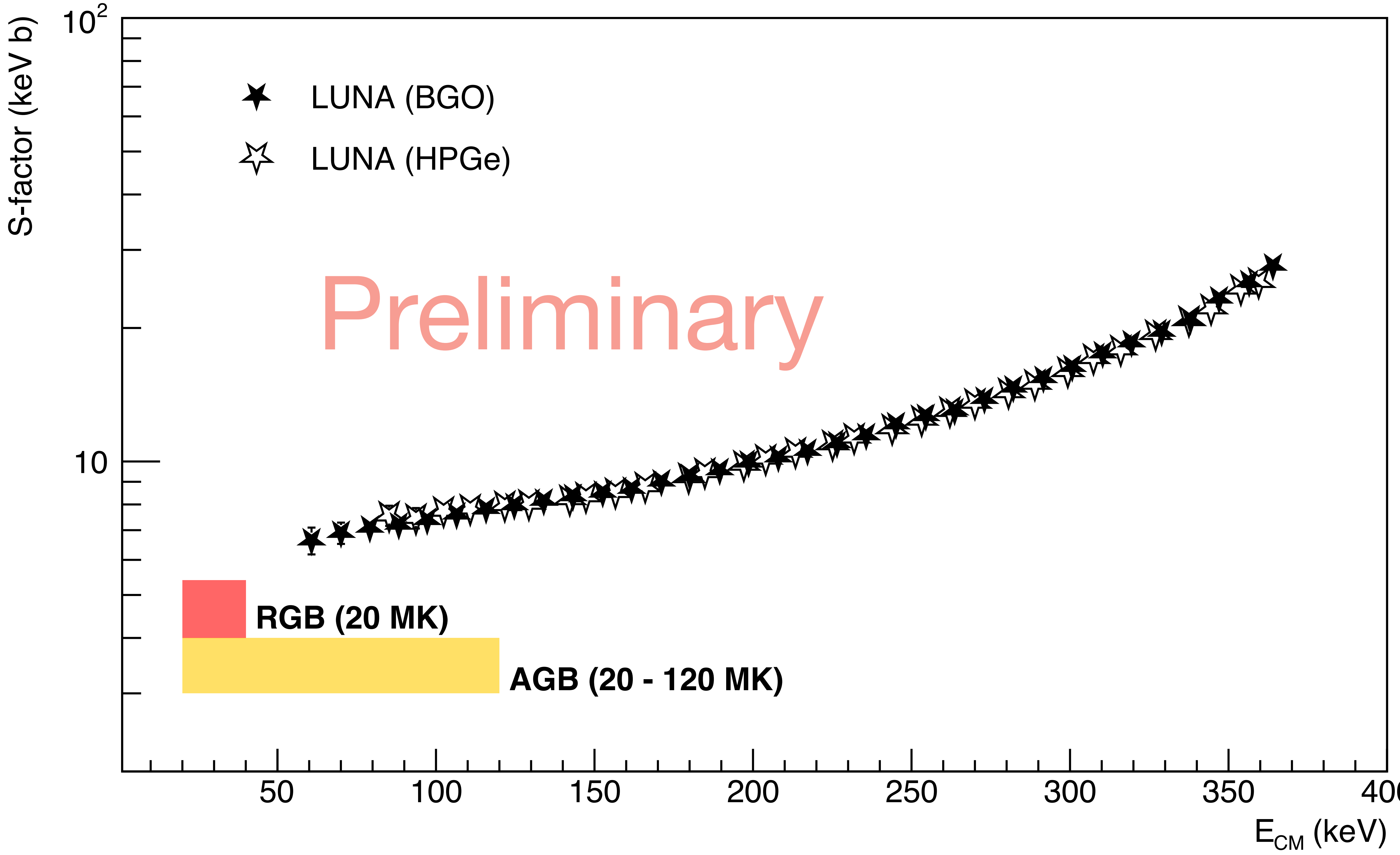

R-Matrix Analysis

- **R-Matrix fits** were performed with **AZURE2** + **BRICK**
- All the **data normalisation factors** were left **free to vary**
- Both **(p, γ)** and **(p, p)** channels were included

$^{12}C(p,\gamma)^{13}N$

- 5 literature datasets for **(p, γ) + LUNA**
- 1 literature dataset for **(p, p)**
- 1 transition
- 2 resonances
- no background poles + ANC from lit

$^{13}C(p,\gamma)^{14}N$

- 5 literature datasets for **(p, γ) + LUNA**
- 1 literature dataset for **(p, p)**
- 6 transitions
- 2 resonances
- no background poles + ANC from lit

R-Matrix - $^{12}C(p,\gamma)^{13}N$ Result

Total Capture

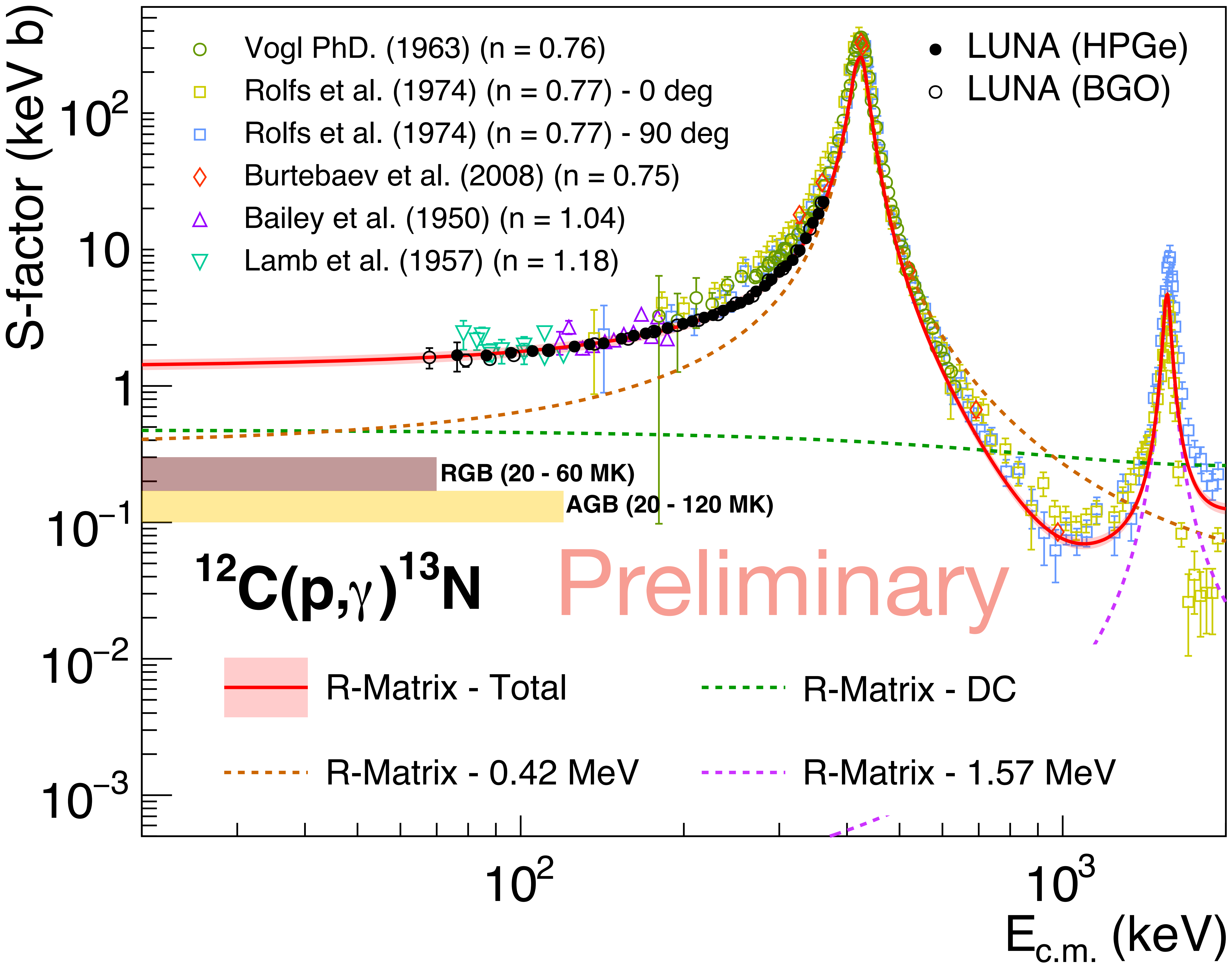

Reaction Rate

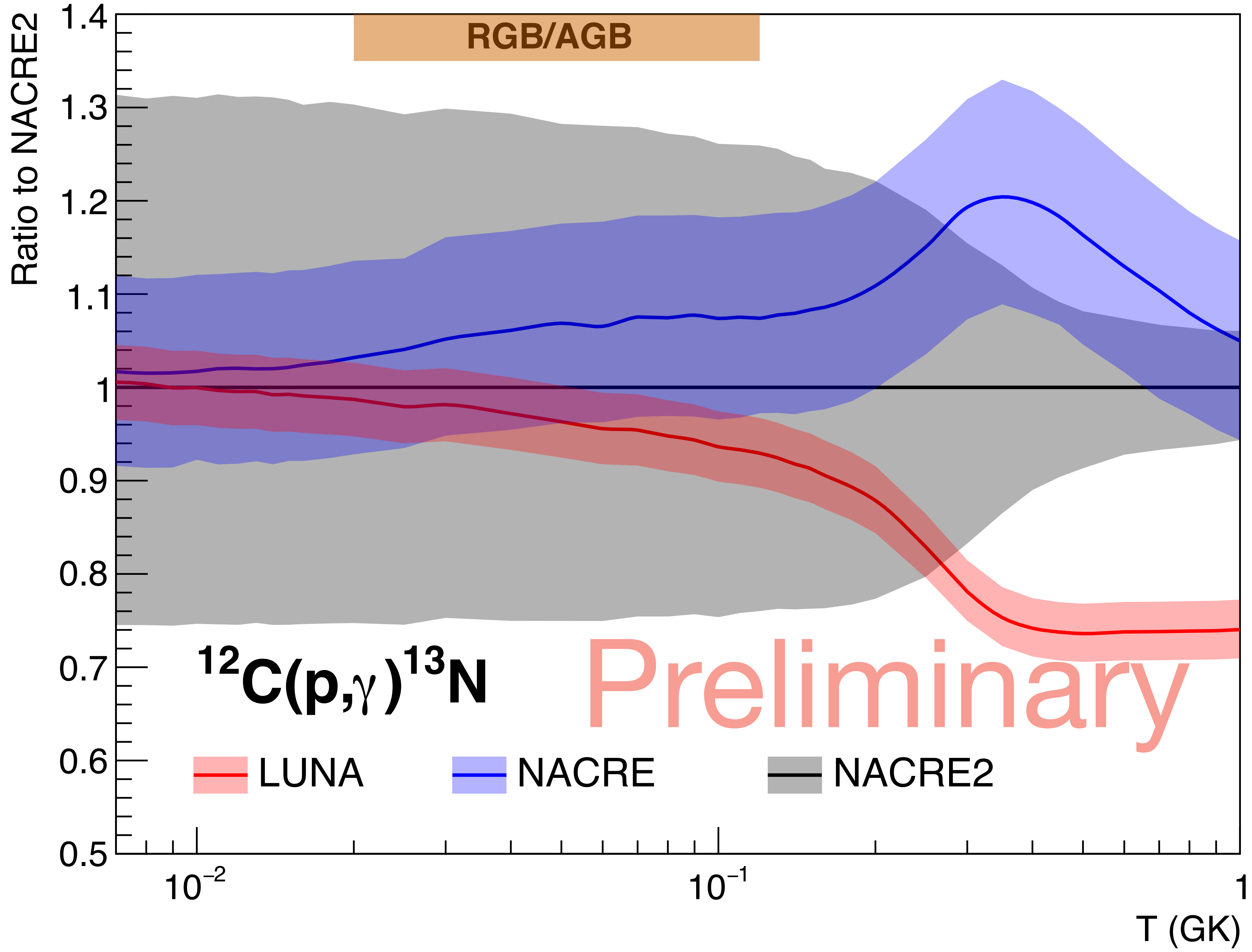

LUNA

R-Matrix - $^{13}C(p,\gamma)^{14}N$ Result

Total Capture

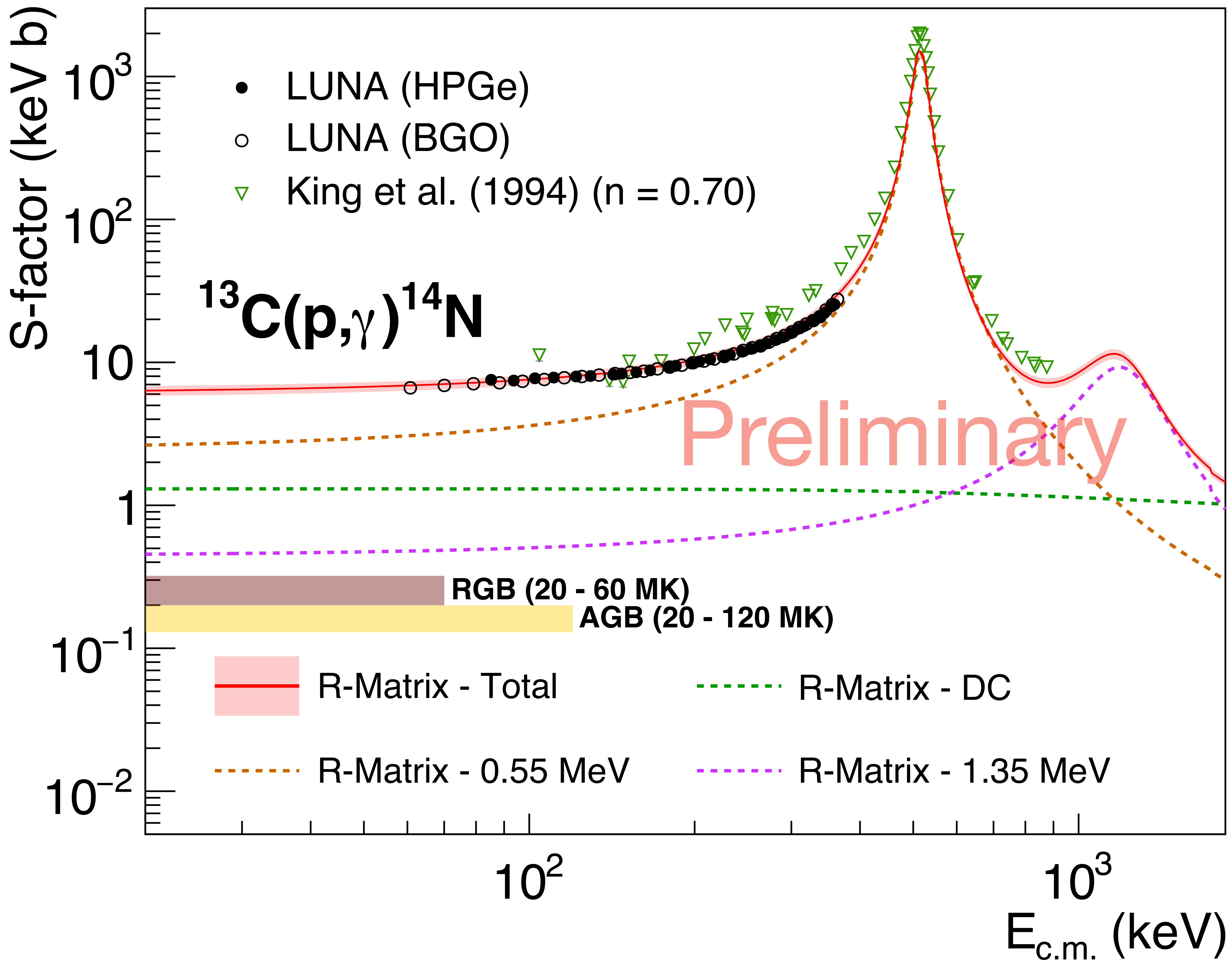

Reaction Rate

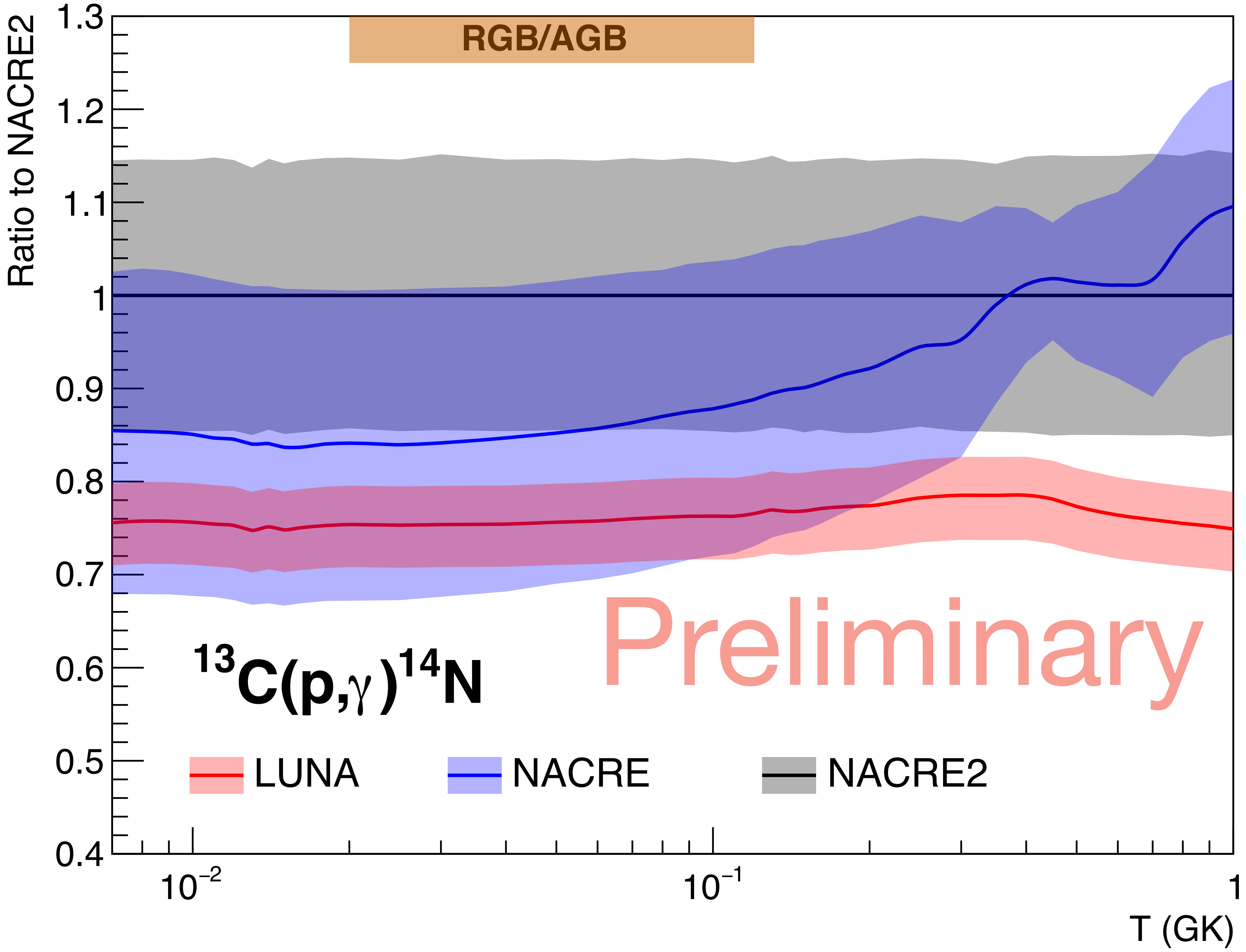

Conclusions

- Both the ^{12}**C(p,γ)**^{13}**N** and ^{13}**C(p,γ)**^{14}**N** cross section were measured at **LUNA**
- Several different techniques and two experimental setups were used
- Systematic uncertainty of **7 - 9 %** was reached (**stopping power** dominated)
- A **complete R-Matrix** analysis was performed with all the literature data
- The new data permitted much **more precise extrapolations** at stellar energies

Thank you for attention!

LUNA Collaboration

R. Perrino | INFN Lecce

A. Formicola | INFN Roma

M. Campostrini, V. Rigato | INFN LNL

O. Straniero | Osservatorio Astronomico di Collurania

F. Cavanna, P. Colombetti | Università di Torino and INFN Torino

A. Compagnucci, F. Ferraro, R. Gesué, M. Junker | INFN LNGS

M. Lugaro | Konkoly Observatory, Hungarian Academy of Sciences

D. Bemmerer, E. Masha | Helmholtz-Zentrum Dresden-Rossendorf

R. Depalo, A. Guglielmetti | Università degli Studi di Milano and INFN Milano

F. Casaburo, S. Zavatarelli | Università degli Studi di Genova and INFN Genova

F. Barile, G.F. Ciani, V. Paticchio, L. Schiavulli | Università degli Studi di Bari and INFN Bari

M. Aliotta, L. Barbieri, C.G. Bruno, J. Marsh, D. Robb, R.S. Sidhu | University of Edinburgh

Z. Elekes, Zs. Fülöp, Gy. Gyürky, L. Csedreki, T. Szücs | Institute of Nuclear Research, ATOMKI

C. Broggini, A. Caciolli, P. Marigo, R. Menegazzo, D. Piatti, J. Skowronski | Università degli Studi di Padova and INFN Padova

C. Ananna, A. Best, D. Dell'Aquila, A. Di Leva, G. Imbriani, D. Mercogliano, D. Rapagnani | Università degli Studi di Napoli and INFN Napoli

$^{12}C/^{13}C$ Ratio

$^{12}C/^{13}C$ Ratio

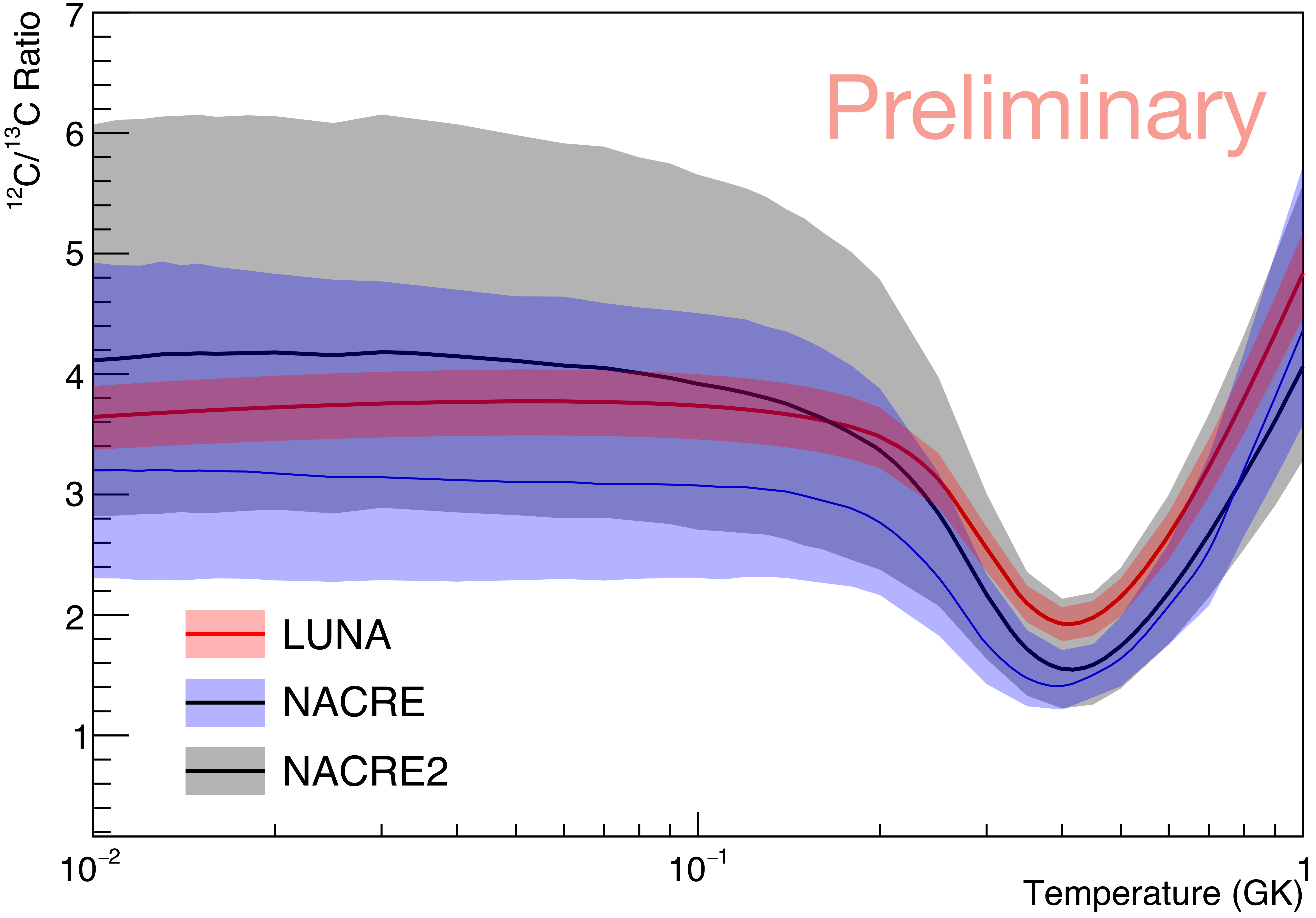

- **Calculated**: 3.6 ± 0.4
- **RGB Metal Poor**: 3 - 6 [1]
- **RGB Giants:** 8 - 14 [1]
- **RGB Model (no mixing):** 27 [2]
- **RGB Model (mixing):** 10 [2]

Lower predicted ratio

↓

Lower mixing needed

[1] M. D. Shetrone (1996), Astron. J., Vol. 112, N. 6
[2] L. Szigeti et al. (2018), MNRAS 474, 4810–4817

HPGe Measurement

Peak Shape Analysis

- The shape of the **γ-peak** is influenced by the **target thickness** and the reaction **cross-section**
- By **parametrising the γ-peak** it is possible to extract both **target** and **cross-section** information

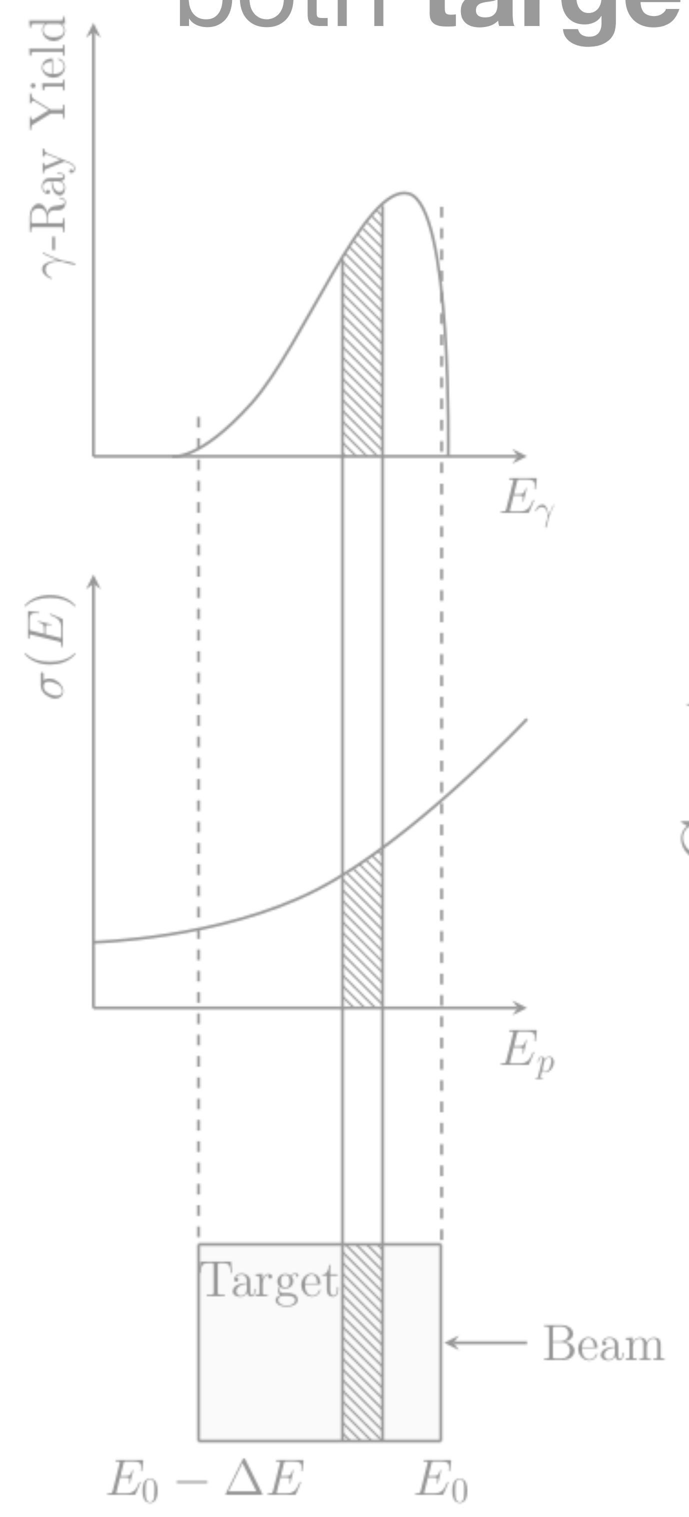

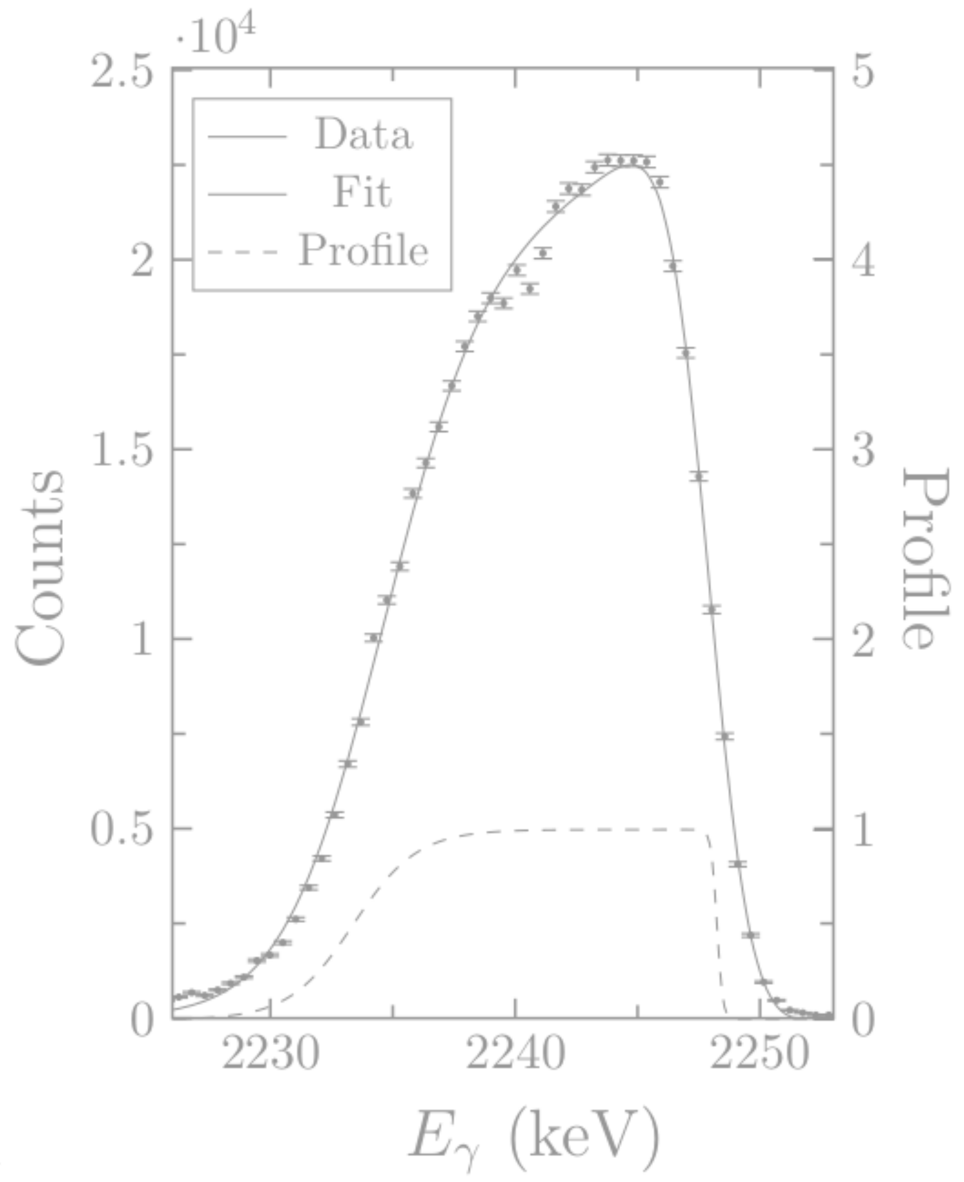

Target: evaporated (ΔE ~ 10 keV)

Energies: 80 - 400 keV

Systematic: 7.1%

All the $^{13}C(p,\gamma)^{14}N$ transitions could be studied

Target Profile Check

- **NRRA scans** of the targets after the measurements
- The **$^{13}C(p,\gamma)^{14}N$** narrow resonance at **1.747 MeV** was used
- The **target profiles** obtained from the Peak Shape Analysis were used for the fit

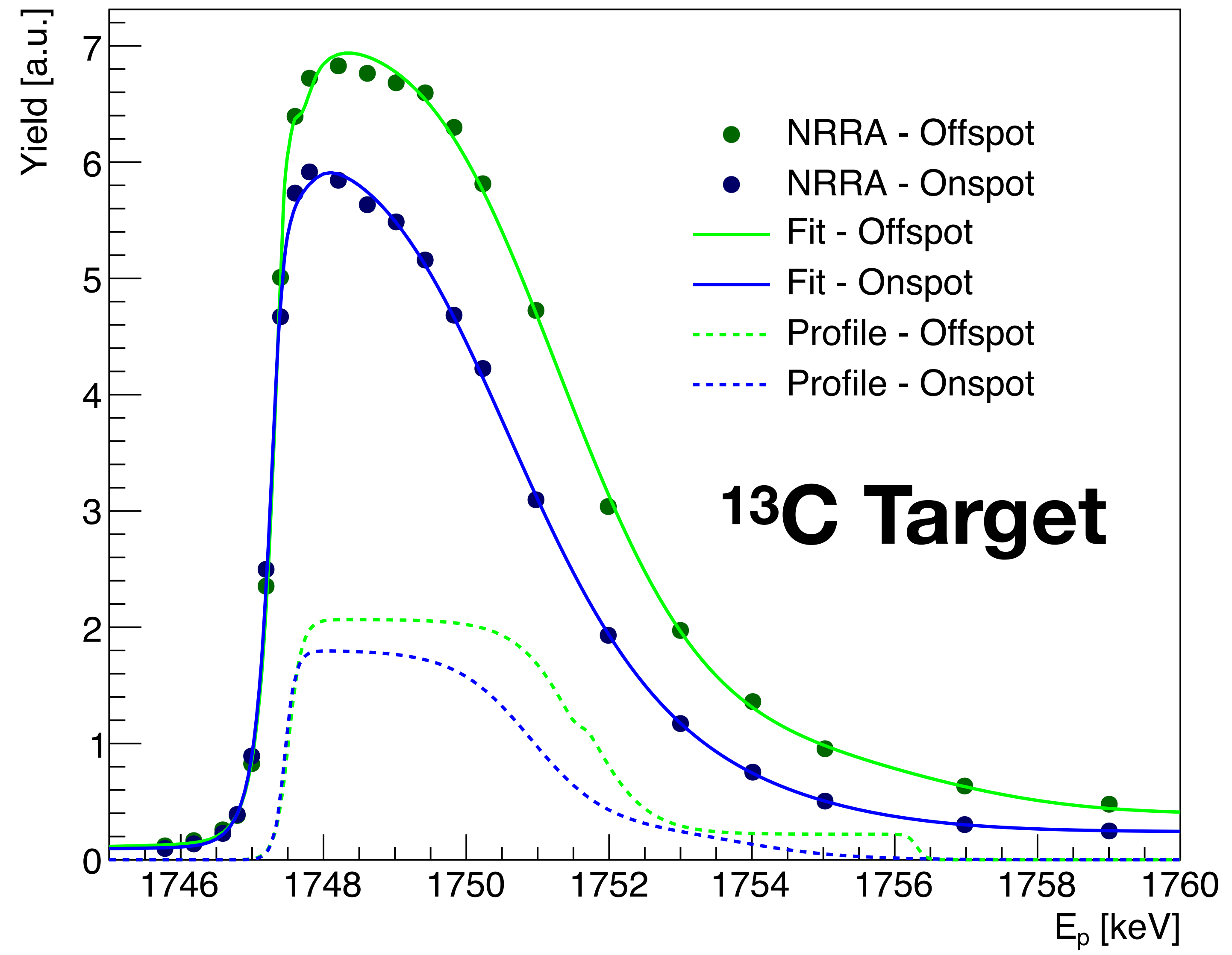

Systematic Uncertainty

$^{12}C(p,\gamma)^{13}N$ - HPGe

Source	Percentage
Efficiency	2 %
Stopping [56]	6.4 %
Target	1.2 %
Total	6.8 %

$^{13}C(p,\gamma)^{14}N$ - HPGe

Source	Percentage
Efficiency	2.6 %
Stopping [56]	6.4 %
Target	1.7 %
Total	7.1 %

$^{12}C(p,\gamma)^{13}N$ - BGO

Source	Percentage
Efficiency	4 %
Stopping [56]	6.4 %
Target	1 %
Beamspot	3 %
Total	8.2 %

$^{13}C(p,\gamma)^{14}N$ - BGO

Source	Percentage
Efficiency	4 %
Stopping [56]	6.4 %
Target	2 – 0.5 %
Beamspot	1.4 %
Branching	0.5 %
Total	7.8 – 7.6 %

Dominated by the **stopping power** uncertainty

LUNA

HPGe Efficiency

- **Multi-parametric fit**
- Sources: ^{60}Co, ^{137}Cs
- Reactions: ^{14}N(p,γ), ^{27}Al(p,γ)
- Uncertainty with **Monte Carlo**

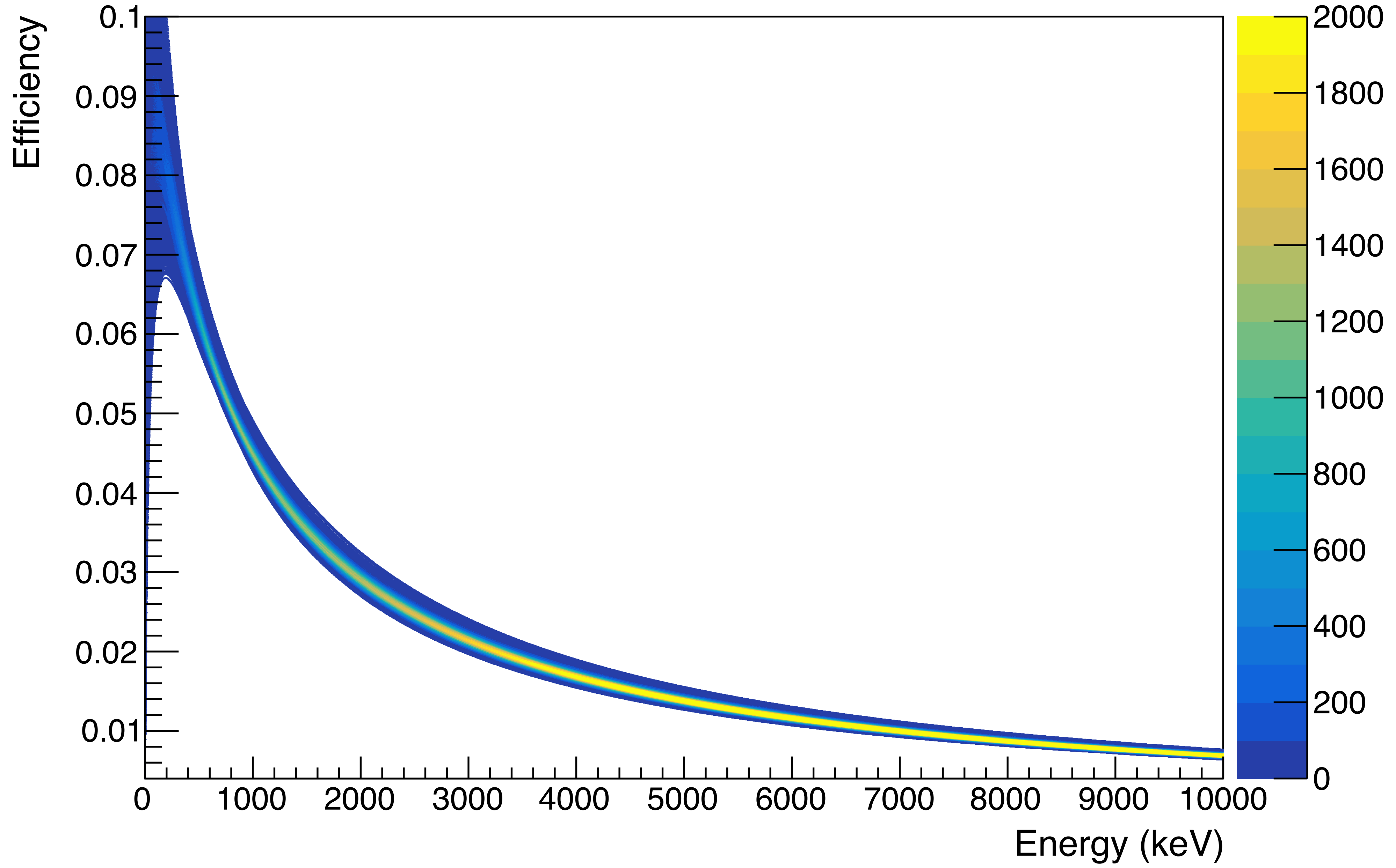

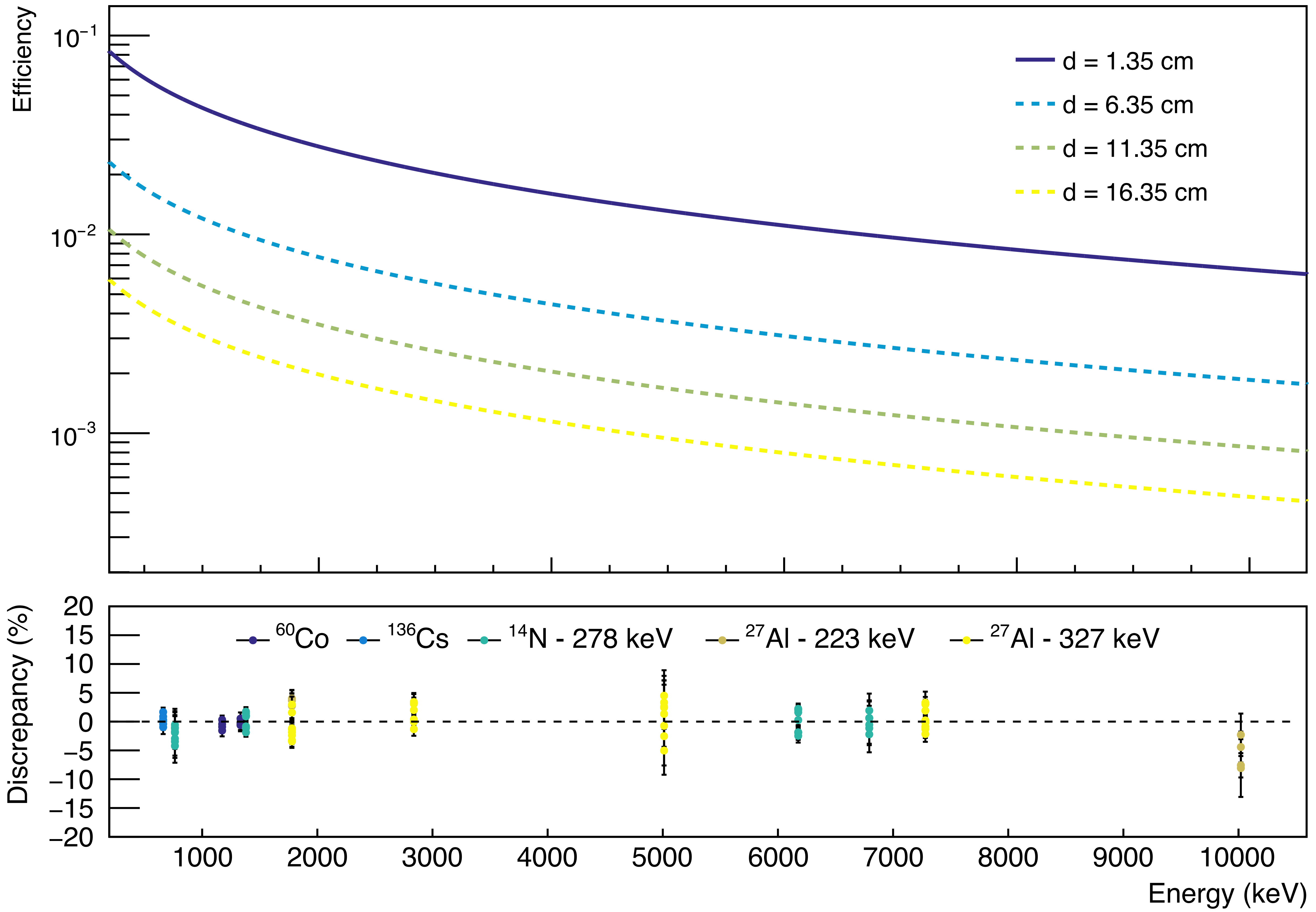

$$\eta_{ph}(d, E_\gamma) = D(d, E_\gamma) \exp\left[a + b\ln(E_\gamma) + c\ln^2(E_\gamma)\right]$$

$$\ln\left(\frac{\eta_{ph}}{\eta_{tot}}\right) = k_1 + k_2\ln(E_\gamma) + k_3\ln^2(E_\gamma)$$

LUNA

BGO Efficiency

- **Geant4** simulations
- Validation with ^{60}Co, ^{137}Cs, ^{14}N(p,γ), ^{27}Al(p,γ)

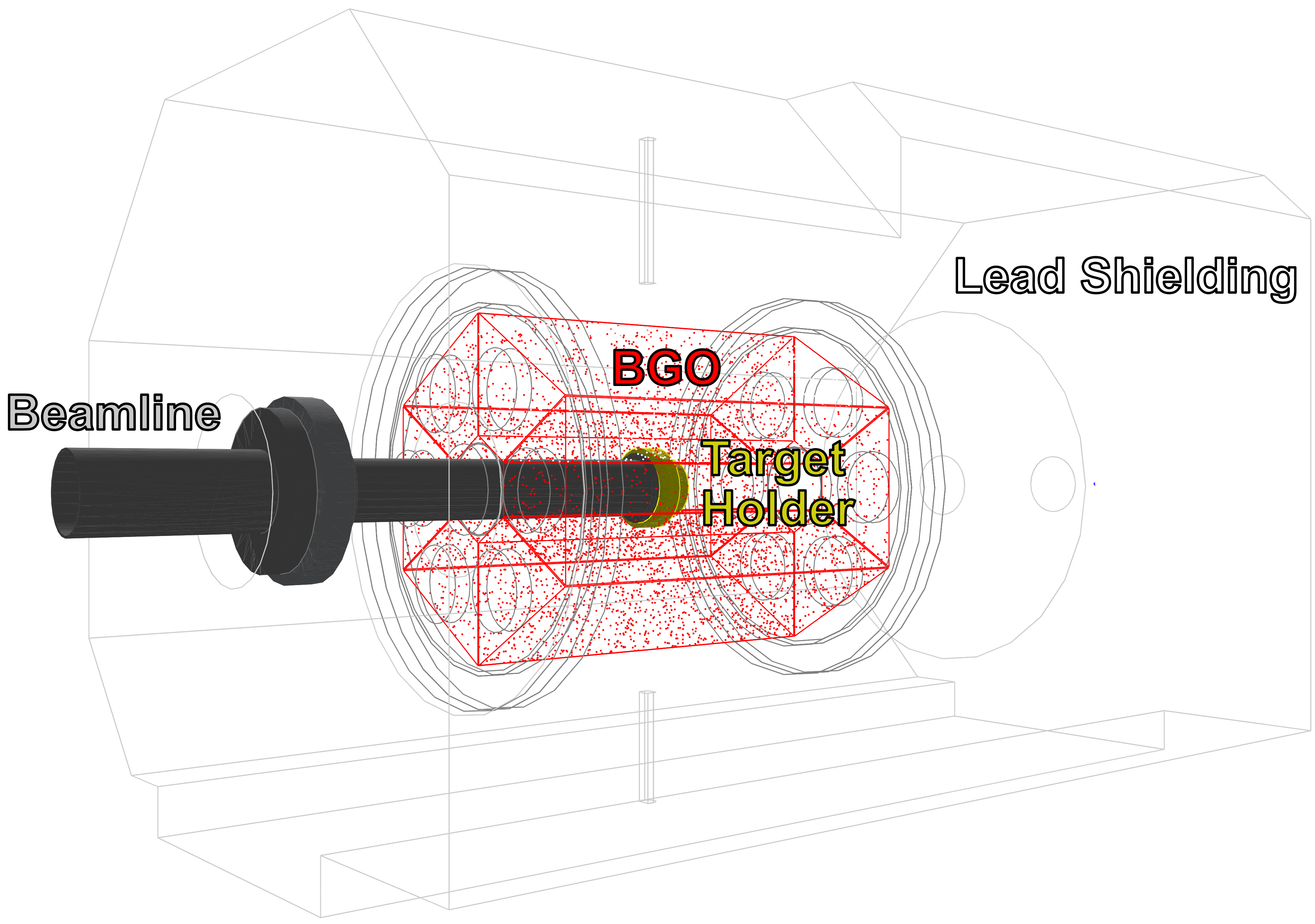

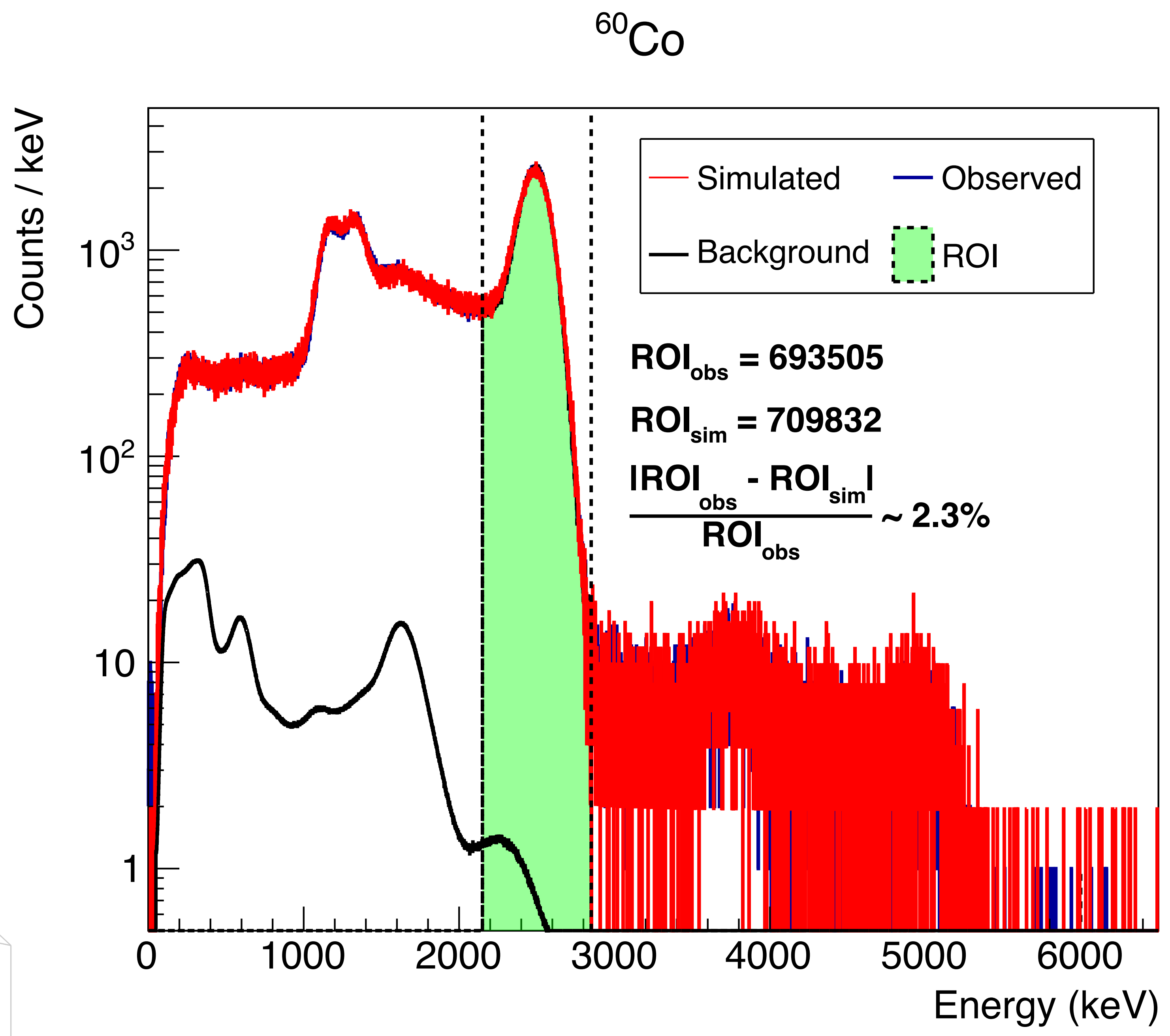

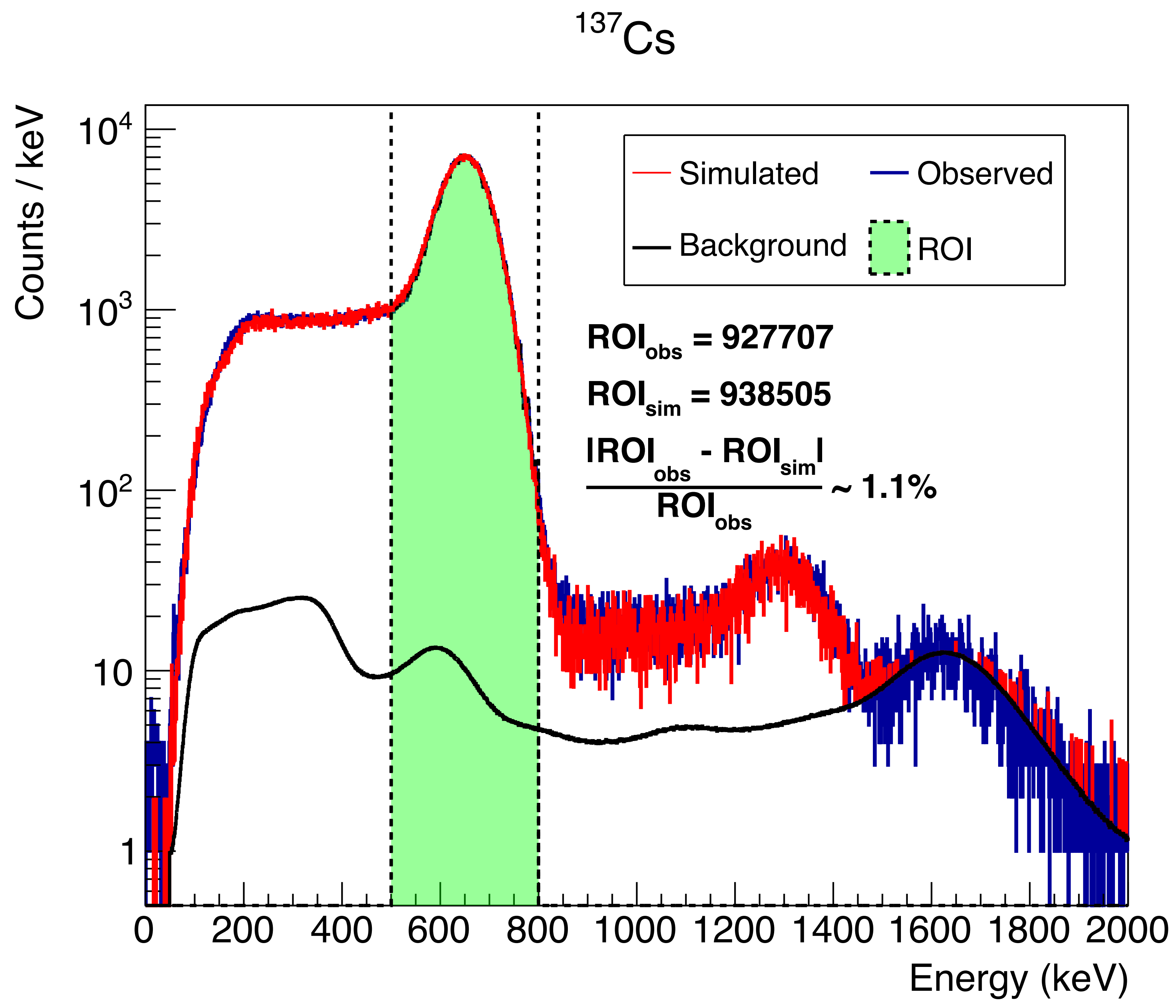

More details in the recently published

J. Skowronski et al. (2023), J. Phys. G: Nucl. Part. Phys. **50** 045201

LUNA

R-Matrix Parameters - $^{12}C(p,\gamma)^{13}N$

- **Lower Γ_γ** for the first broad resonance
- **Higher Γ_p** for the second broad resonance

Source	E_r (keV)	Γ_p (keV)	Γ_γ (eV)
Literature	461 ± 1	33.5 ± 1	0.63 ± 0.07
Frequentist	460.6 ± 0.2	34.5 ± 0.2	0.46 ± 0.02
Bayesian	458.9 ± 0.3	33.5 ± 0.2	0.43 ± 0.02

Table 4.11: The 2365 keV resonance parameters for the fit of the $^{12}C(p,\gamma)^{13}N$.

Source	E_r (keV)	Γ_p (keV)	Γ_γ (eV)
Literature	1706 ± 1	46.0 ± 3.4	0.35 ± 0.08
Frequentist	1689.9 ± 0.3	54.2 ± 0.9	0.37 ± 0.05
Bayesian	1688.6 ± 0.4	54.1 ± 0.4	0.36 ± 0.02

Table 4.12: The 3502 keV resonance parameters for the fit of the $^{12}C(p,\gamma)^{13}N$.

Source	E_r (keV)	Γ_p (keV)
Literature	1735 ± 2	48.3 ± 1.9
Frequentist	1737.0 ± 0.4	49.0 ± 0.9
Bayesian	1735.7 ± 0.5	48.9 ± 0.6

Table 4.13: The 3545 keV resonance parameters for the fit of the $^{12}C(p,\gamma)^{13}N$.

Source	ANC ($fm^{-1/2}$)
Literature	1.64 ± 0.11
Frequentist	1.67 ± 0.04
Bayesian	1.80 ± 0.03

Table 4.14: The ANC parameters for the fit of the $^{12}C(p,\gamma)^{13}N$.

Bayesian and frequentist mostly in agreement

LUNA

R-Matrix Parameters - $^{13}C(p,\gamma)^{14}N$

- **Lower Γ_γ** for the first broad resonance

- Second broad resonance is **poorly constrained**

Reference	E_r (keV)	Γ_p (keV)	Γ_γ (eV)					
			R $\to$ 0 keV	R $\to$ 2312 keV	R $\to$ 3948 keV	R $\to$ 4915 keV	R $\to$ 5105 keV	R $\to$ 5691 keV
Literature	557 ± 3	37.2 ± 0.3	9.09 ± 0.05	0.22 ± 0.04	1.544 ± 0.009	0.26 ± 0.01	0.074 ± 0.008	0.612 ± 0.006
Frequentist	557.2 ± 0.2	36.5 ± 0.3	6.26 ± 0.32	0.14 ± 0.02	1.36 ± 0.08	0.26 ± 0.02	0.047 ± 0.004	0.51 ± 0.03
Bayesian	557.3 ± 0.1	36.7 ± 0.2	6.31 ± 0.36	0.14 ± 0.01	1.40 ± 0.09	0.23 ± 0.01	0.050 ± 0.006	0.49 ± 0.03

Table 4.27: The 8062 keV resonance parameters for the fit of the $^{13}C(p,\gamma)^{14}N$.

Reference	E_r (keV)	Γ_p (keV)	Γ_γ (eV)			
			R $\to$ 0 eV	R $\to$ 3948 eV	R $\to$ 5105 eV	R $\to$ 5691 eV
Literature	1347	460	40.96	0.556	0.23	0.23
Frequentist	1380 ± 6	500 ± 13	30 ± 2	4.8 ± 2.4	0.7 ± 0.7	2.5 ± 0.9
Bayesian	1371 ± 8	500 ± 6	30 ± 2	0.6 ± 0.4	0.8 ± 0.3	1.8 ± 0.02

Table 4.28: The 8776 keV resonance parameters for the literature fit of the $^{13}C(p,\gamma)^{14}N$.

Source	ANC ($fm^{-1/2}$)								
	0 keV ($s=0$)	0 keV ($s=1$)	2312 keV	3948 keV ($s=0$)	3948 keV ($s=1$)	4915 keV	5105 keV ($s=0$)	5105 keV ($s=1$)	5691 keV
Literature	1.68 ± 0.12	4.03 ± 0.13	2.98 ± 0.15	0.98 ± 0.03	1.39 ± 0.04	5.74 ± 0.33	0.49 ± 0.02	0.40 ± 0.02	3.21 ± 0.11
Frequentist	3.33 ± 0.27	3.03 ± 0.19	2.82 ± 0.17	2.61 ± 0.34	1.16 ± 0.09	4.26 ± 0.16	0.67 ± 0.12	0 ± 3	3.28 ± 0.11
Bayesian	2.50 ± 0.23	2.70 ± 0.14	2.62 ± 0.13	0.85 ± 0.39	1.20 ± 0.06	4.58 ± 0.06	0.57 ± 0.07	0.25 ± 0.07	3.34 ± 0.11

Table 4.29: The ANC parameters for the literature fit of the $^{13}C(p,\gamma)^{14}N$.

Discrepancies between Bayesian and frequentist

LUNA

R-Matrix Correlation - $^{12}C(p,\gamma)^{13}N$

Bayesian

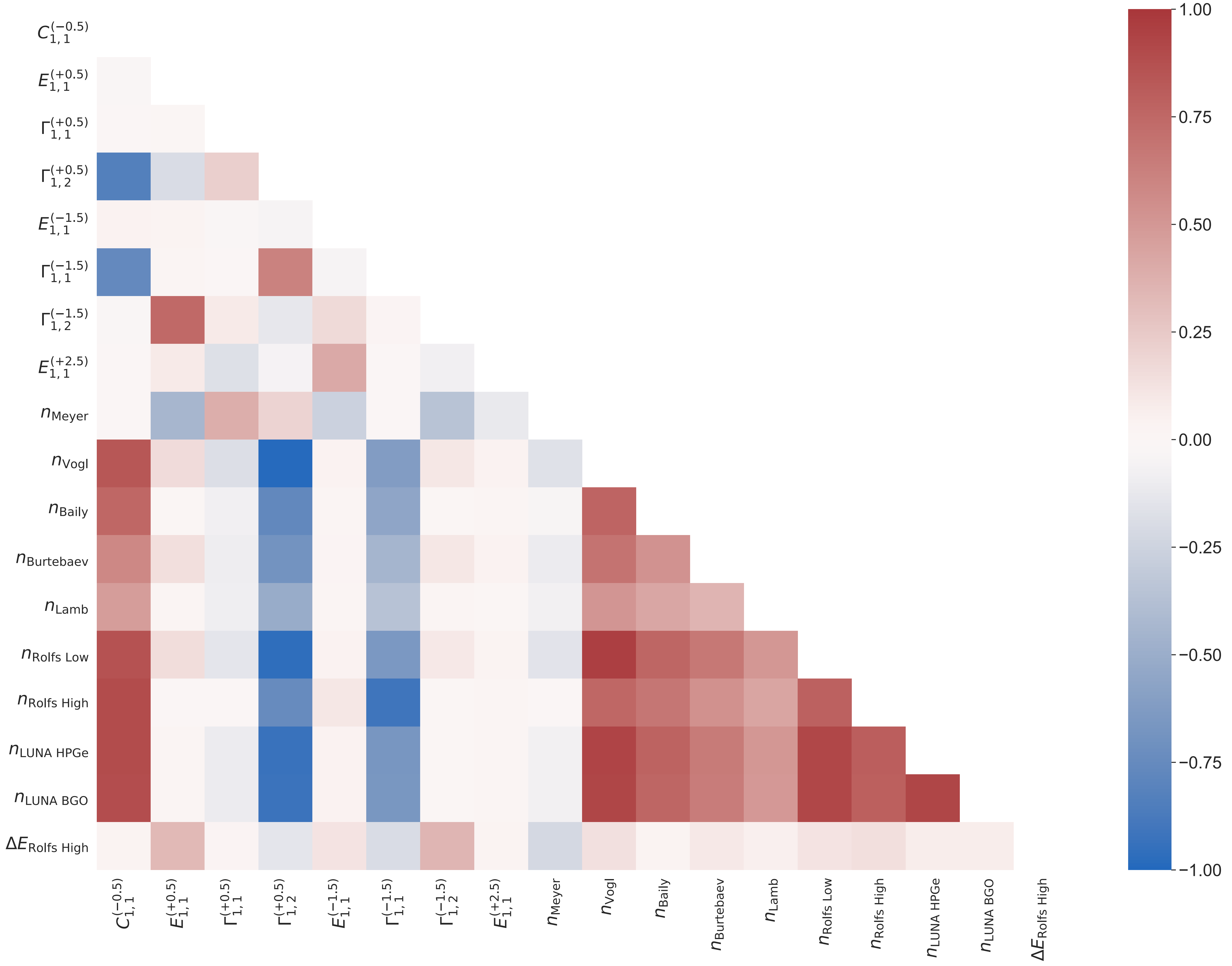

Frequentist

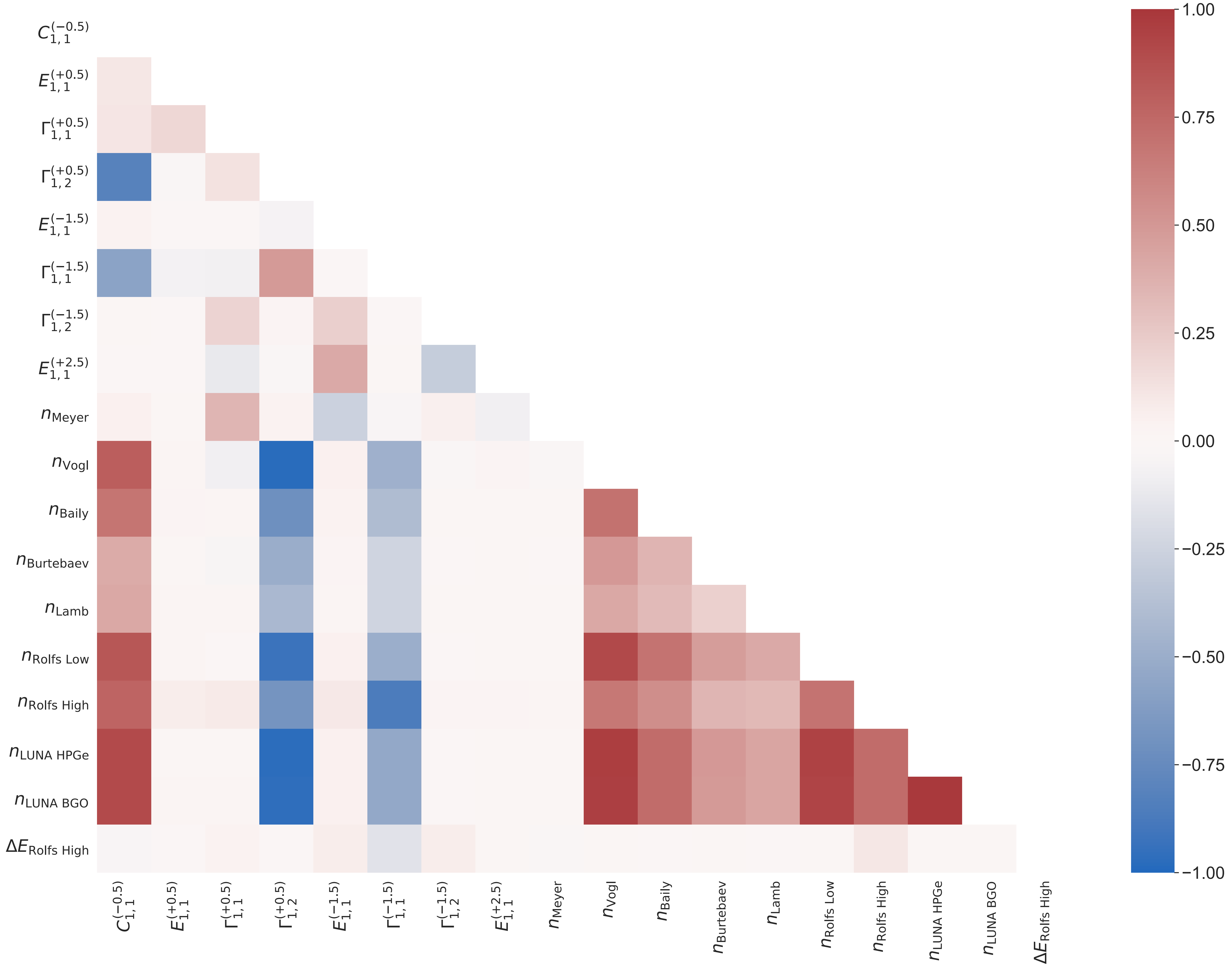

R-Matrix Correlation - $^{13}C(p,\gamma)^{14}N$

Bayesian

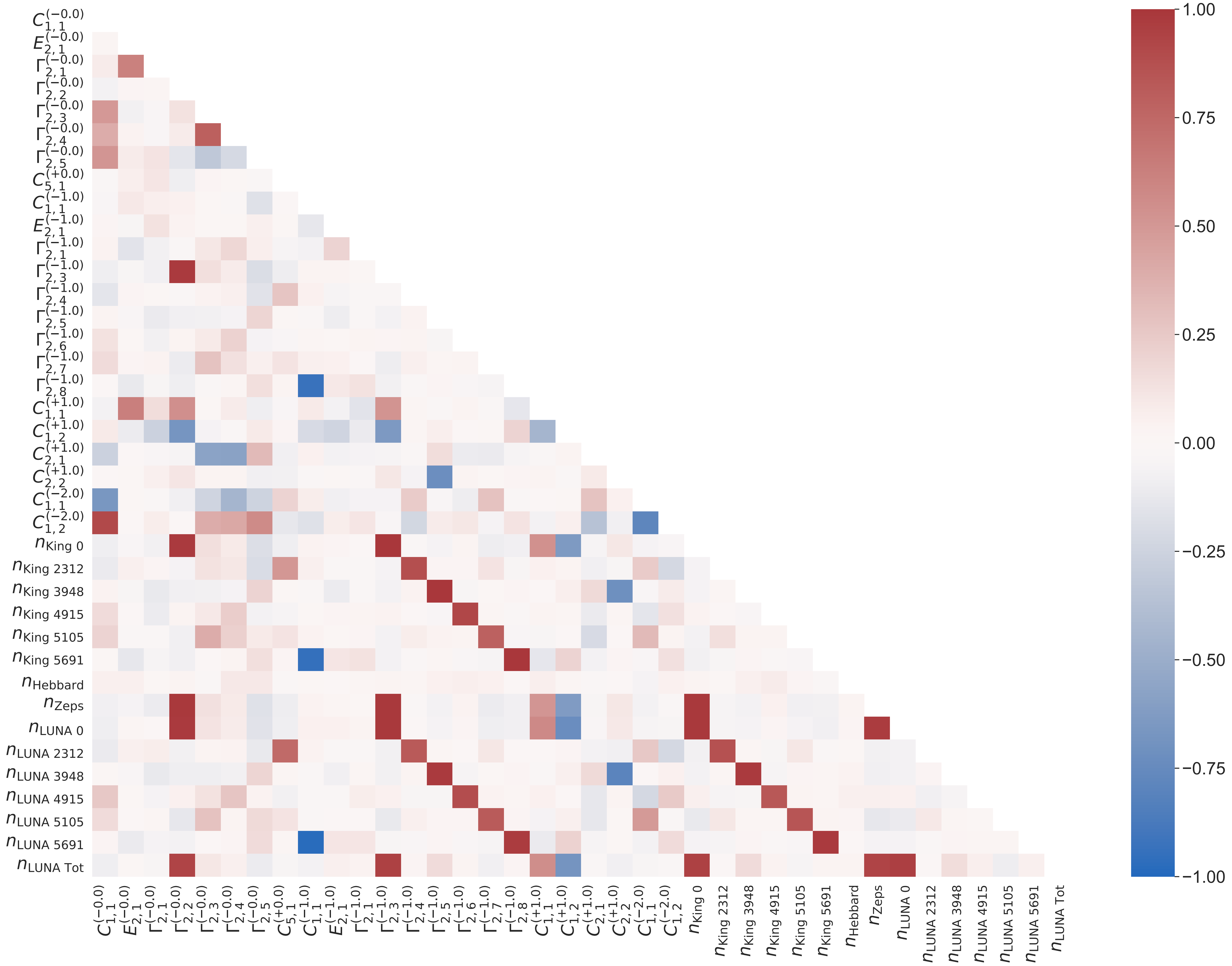

Frequentist

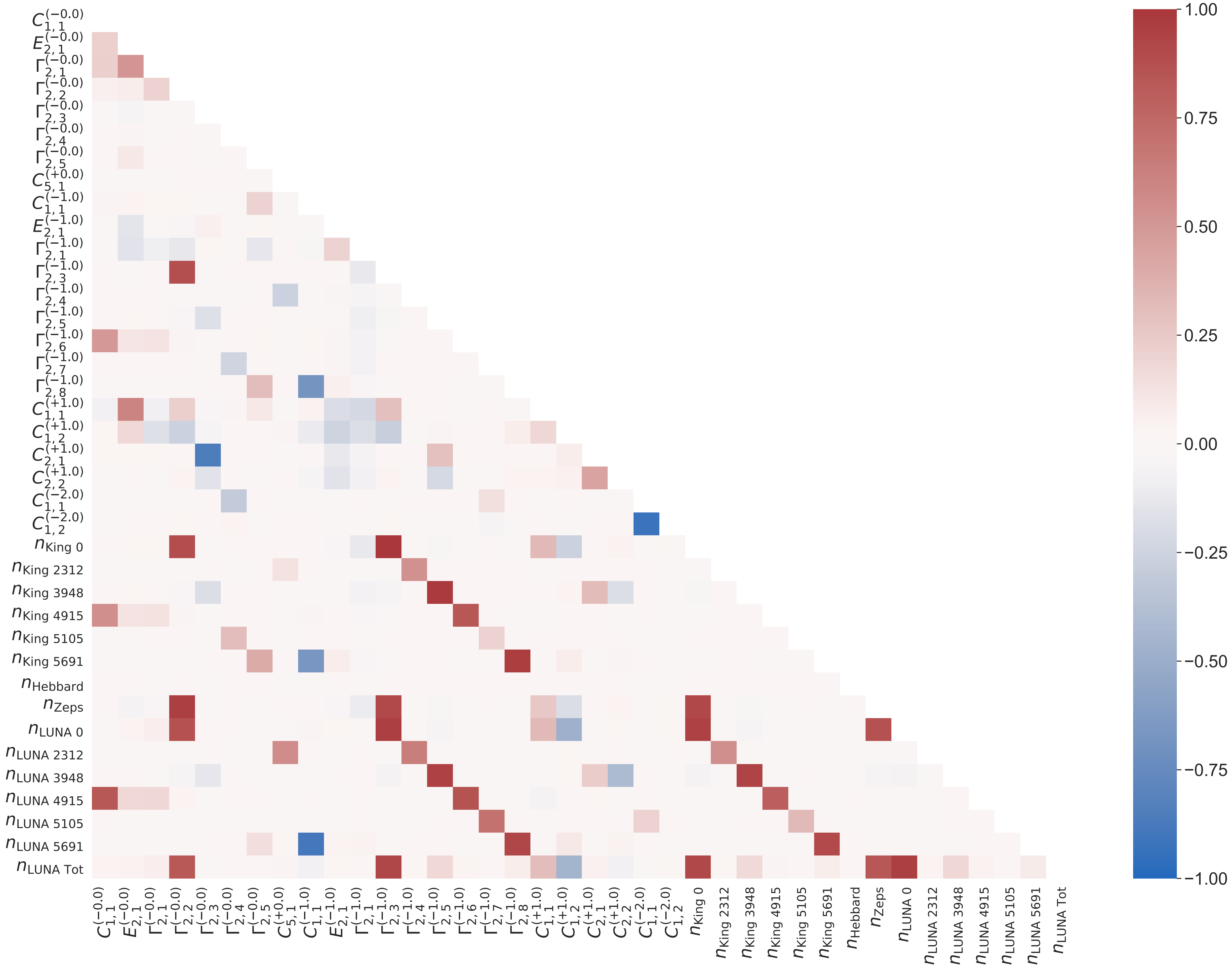

R-Matrix Analysis - Bayesian vs Frequentist

Bayesian

Pros

- Multiple parallel minimisations (with different initial values)
- Easy to include prior information
- More detailed information on parameter distribution
- Straightforward uncertainty

Cons

- Slower

$^{12}C(p,\gamma)^{13}N$ ANC Distributions

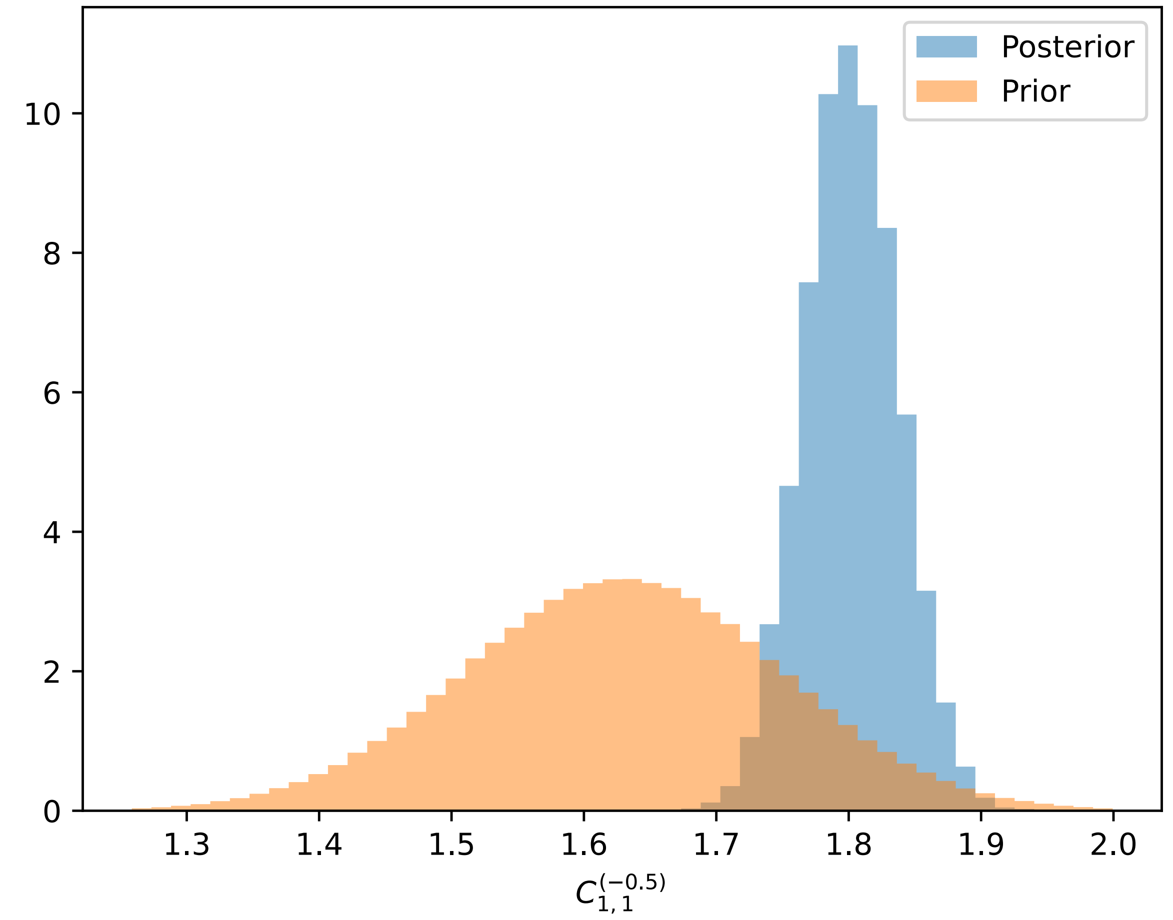

$^{12}C(p,\gamma)^{13}N$ ANC vs Γ_γ Covariance

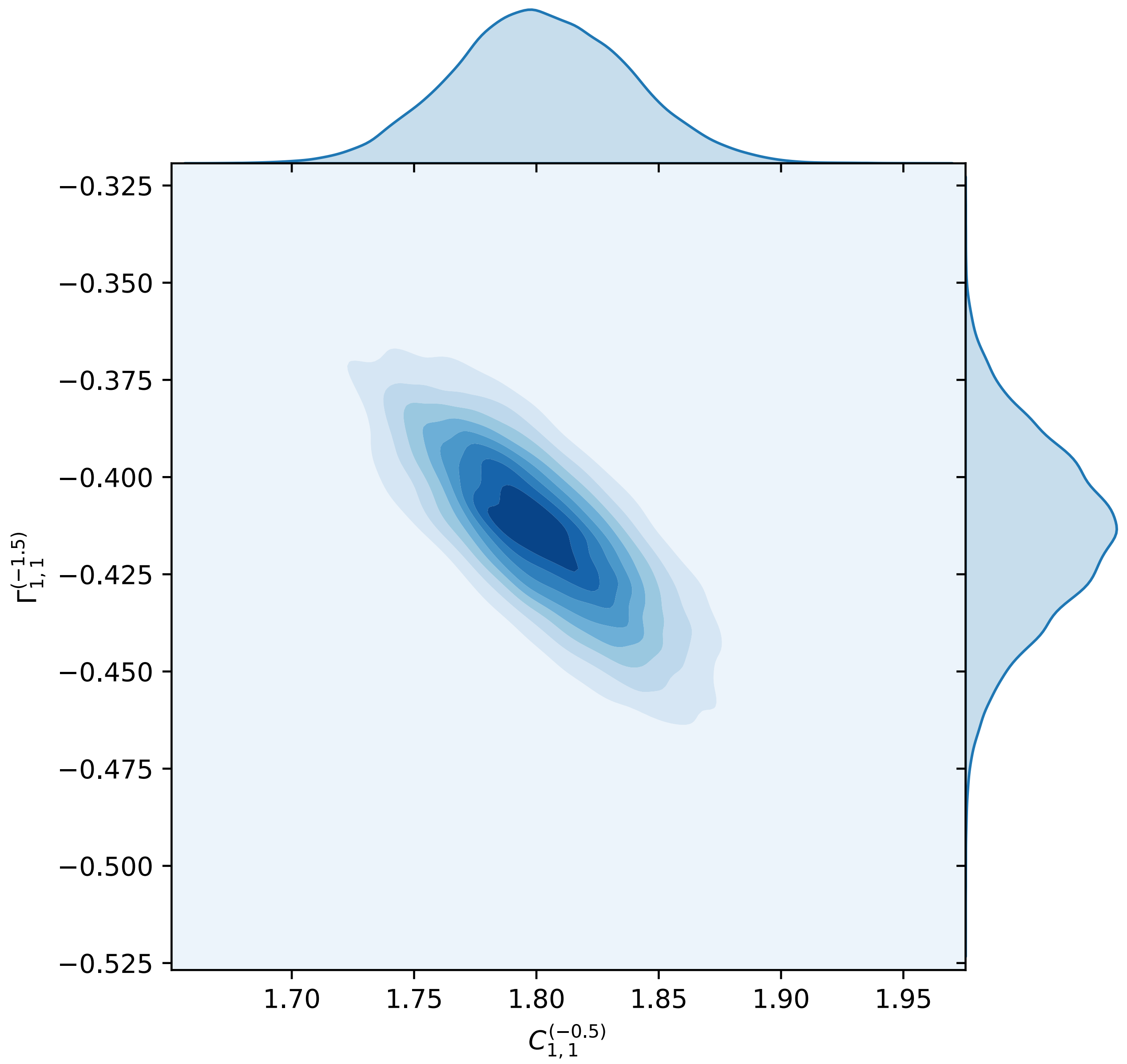

Frequentist

Pros

- Faster
- More used in the community (?)

Cons

- Troublesome uncertainty estimation
- Can hang on a local minimum
- Low covariance
- No easy to include prior information

LUNA